Hydrodynamic theory of vorticity-induced spin transport

Gen Tatara
RIKEN Center for Emergent Matter Science (CEMS) and RIKEN Cluster for Pioneering Research (CPR), 2-1 Hirosawa, Wako, Saitama 351-0198, Japan

(Received 23 August 2021; revised 26 October 2021; accepted 8 November 2021; published 15 November 2021)

Electron spin transport in a disordered ferromagnetic metal is theoretically studied from the hydrodynamic viewpoint, focusing on the role of electron vorticity. The spin-resolved momentum flux density of electrons is calculated microscopically, taking account of the spin-orbit interaction and uniform magnetization, and the expression for the spin motive force is obtained as the linear response to a driving electric field. It is shown that the spin-resolved momentum flux density and motive force are characterized by troidal moments, vector products of the applied external electric field and the spin polarization or magnetization, which act as effective driving fields when the anomalous or spin Hall effects are taken into account. The spin-vorticity and magnetization-vorticity couplings are shown to arise naturally as conservative forces driven by the toroidal moments, and nonconservative forces are also found to exist. Spin accumulation induced by the electron flow is calculated and vorticity-induced torque and spin relaxation are discussed. The vorticity-induced torque, a linear effect of the spin-orbit interaction, is argued to be larger than the conventional relaxation torques acting on magnetization structures such as nonadiabatic (β) current-induced torque. The direct and inverse spin Hall effects and spin-orbit torque are discussed in the context of spin-vorticity coupling.

DOI: 10.1103/PhysRevB.104.184414

I. INTRODUCTION

Electron transport in magnetic metals has been studied in various systems. Technologically, the most successful effect would be the giant magnetoresistance (GMR) effect discovered in magnetic layers [1]. GMR effects in multilayers were theoretically described based on a two-current electron model derived from the Boltzmann equation for the conduction electrons with spin up and down [2]. Mutual effects of magnetic structures and electron transport have been argued in the context of magnetoresistance and spin-transfer torque [3–7]. In previous works on spin transport, effects of nonuniform magnetization were focused on, while current density was treated as uniform. In reality, however, the current is inhomogeneous at the edges, inducing local vorticity of electron flow. Vorticity of current density $\boldsymbol{j}$, $\boldsymbol{\omega}_{\rm e} \equiv \nabla\times\boldsymbol{j}$, carries angular momentum and can couple to the magnetic field and spin, affecting local spin transport. In fact, an electron's vorticity was shown theoretically to couple to electron spin via a quantum relativistic effect called the spin-vorticity coupling [8], and various phenomena induced by the coupling have been discussed recently [9–12].

A. Spin, magnetization, and vorticity

Spin-vorticity coupling of electrons is represented by an energy proportional for the spin $\boldsymbol{s}$ and vorticity $\boldsymbol{\omega}_{\rm e}$, $\mathcal{E}_{\rm sv} = -\zeta_{\rm sv}\boldsymbol{s}\cdot\boldsymbol{\omega}_{\rm e}$, where $\zeta_{\rm sv}$ is a coefficient. For a macroscopic number of spins as an ensemble, the coupling reduces to a magnetization($\boldsymbol{M}$)-vorticity coupling, $\mathcal{E}_{M\rm v} = -\zeta_{M\rm v}\boldsymbol{M}\cdot\boldsymbol{\omega}_{\rm e}$, where $\zeta_{M\rm v}$ is a coefficient. The coupling indicates the equivalence of mechanical rotation and magnetization, which was argued in 1915 by Barnett [13] and Einstein and de Haas [14]. The spin-vorticity coupling was phenomenologically argued in the context of hydrodynamic coefficients by Snider and Lewchuk [15], and vorticity was argued to act as a source for spin density. In the recent context of spintronics, the spin-vorticity coupling was derived from the Dirac equation in a rotating frame by Matsuo *et al.* [8], and mechanical spin current generation effect was argued [16]. The spin-vorticity coupling induces a force on the electron spin (spin motive force) proportional to $\nabla(\boldsymbol{s}\cdot\boldsymbol{\omega}_{\rm e})$. This force is theoretically identified below in the hydrodynamic approach, calculating the momentum flux density [see Eqs. (23) and (24)]. Experimental evidence of the effect was reported in mercury liquid [17]. In Ref. [11], microscopic calculation of stress tensors for electron spin was carried out in the nonmagnetic case and spin-vorticity coupling was shown to arise from the spin-orbit interaction.

It was demonstrated recently [18] that the spin Hall effect, an electric generation of spin current [19,20], is explained by the spin-vorticity coupling. In fact, the spin density induced by the spin Hall effect in a clean conductor was shown to be

$$\boldsymbol{s} = \lambda_{\rm sh}\boldsymbol{\omega}, \tag{1}$$

where $\boldsymbol{\omega} \equiv \nabla\times\boldsymbol{E}$ is a vorticity of the applied electric field and $\lambda_{\rm sh}$ is a constant arising from the spin-orbit interaction [18]. This relation is equivalent to the spin-vorticity coupling at the lowest order in the spin-orbit interaction due to the local relation between $\boldsymbol{j}$ and $\boldsymbol{E}$.

The effect of an external magnetic field on electron fluid was studied theoretically and the Hall viscosity was discussed in Refs. [21,22]. The Hall viscosity, the Hall component of the viscosity tensor, η_{xy}, represents a force $\boldsymbol{f}^{\rm H} = \eta_{xy}\hat{\boldsymbol{B}}\times\nabla^2\boldsymbol{j}$ ($\hat{\boldsymbol{B}}$ is the direction of the magnetic field). Using $\nabla^2\boldsymbol{j} = -\nabla\times\boldsymbol{\omega}_{\rm e} + \nabla(\nabla\cdot\boldsymbol{j})$ and focusing on the effect of vorticity $\boldsymbol{\omega}_{\rm e}$, the diagonal component of the corresponding momentum flux density $\pi^{\rm H}_{ij}$ ($f^{\rm H}_i = -\nabla_j\pi^{\rm H}_{ij}$) turns out to be $\pi^{\rm H(diag)}_{ij} = \delta_{ij}\eta_{xy}(\hat{\boldsymbol{B}}\cdot\boldsymbol{\omega}_{\rm e})$; namely, the Hall viscosity arises from the magnetic field-vorticity coupling.

Therefore, previous studies indicate that a magnetic field, a magnetization, and a spin couples to the electron vorticity in the same manner as is naturally expected from symmetry [15].

B. Ohmic electron fluid and scope of the paper

Vorticity arises generally near surfaces and interfaces where longitudinal flow is suppressed, and vorticity-induced effects are expected to dominate various transport properties in thin films and mesoscopic systems. For discussing vorticity effects, hydrodynamic equations are useful to identify the forces due to inhomogeneity of the flow. Electron transport in metals with disorder is governed by relaxation force instead of viscosity force in conventional fluids. Coarse-grained behaviors of such disordered metals are described in terms of an ohmic fluid [23]. A thorough study of two-dimensional electron fluid in the viscous and ohmic regimes was carried out focusing on the boundary effects in Ref. [24]. Hydrodynamic description of ohmic electron fluid was employed to describe angular momentum generation in spin transport [11,25], chiral electron systems, and anomalous Hall effect [26,27]. Hydrodynamic equations are conventionally represented in terms of current density $\boldsymbol{j}$. In ohmic fluids, electric current density is locally related to a driving electric field $\boldsymbol{E}$ as $\boldsymbol{j} = \sigma_{\rm e}\boldsymbol{E}$, where $\sigma_{\rm e}$ is a conductivity tensor. Using the local relation, the hydrodynamic equations can thus be represented in terms of the driving field. In the driving-field representation, hydrodynamic coefficients are directly related to microscopic response functions to the applied field, and are systematically calculable by use of a microscopic linear response theory [26,28].

In this paper, we study spin transport effects from the hydrodynamic viewpoint, focusing on the effects of vorticity. We calculate on microscopic grounds the spin-resolved momentum flux density and spin motive force as a linear response to a spatially inhomogeneous applied electric field.

The spin-vorticity coupling potential induces a force proportional to its gradient, $\nabla(\boldsymbol{s}\cdot\boldsymbol{\omega})$. From the symmetry, another form of the force $(\boldsymbol{s}\cdot\nabla)\boldsymbol{\omega} \equiv \boldsymbol{f}_{\rm nc}$ is allowed. Noting $\nabla\cdot\boldsymbol{\omega} = 0$, $\boldsymbol{f}_{\rm nc} = \nabla\times(\boldsymbol{\omega}\times\boldsymbol{s})$ is a nonconservative force, which is allowed if there is viscosity or friction. We shall demonstrate that such a nonconservative force indeed exists in the present electron spin fluid. In the context of magnetization-vorticity coupling, the same form of a nonconservative force with $\boldsymbol{s}$ replaced by magnetization was identified in Ref. [27].

The spin-vorticity coupling indicates that there are current-induced torques arising from vorticity of current in ferromagnets. The torque arises from the inhomogeneity of current density instead of inhomogeneity of magnetization for conventional current-induced torques argued in the context of spin-transfer torque [7,29]. The effect would be localized near

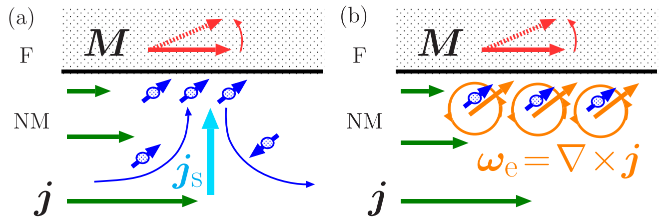

FIG. 1. Two scenarios for the spin Hall-induced spin-orbit torque acting on magnetization $\boldsymbol{M}$ induced by an applied current in a bilayer of ferromagnet (F) and nonmagnetic metal (NM). (a) Conventional picture explaining the torque in terms of spin current ($j_{\rm s}$) generation in NM. (b) In the spin-vorticity picture, spin accumulation is generated directly by the vorticity $\omega_{\rm e}$ created near the interface as a result of suppression of current $\boldsymbol{j}$. They are equivalent, as was argued in Ref. [18].

surfaces and interfaces and is expected to be enhanced by introducing artificial roughness or inhomogeneous structures. We shall demonstrate that the vorticity-induced torque arises theoretically at the linear order of the spin-orbit interaction, while conventional current-induced nonadiabatic torque (β torque) is the second-order effect [7,30]. Moreover, the length scale of vorticity can be controlled by artificial notches and it can be reduced to the order of the electron mean-free path at the smallest. In contrast, the length scale of magnetization structures such as domain wall width is determined by material constants, the exchange and anisotropy energies. In disordered metal with smaller vorticity size compared to the domain wall width, therefore, the vorticity-induced torque is expected to dominate the surface spin-orbit torques. The vorticity-induced torque has a vanishing bulk component, while it acts in thin films as an alternating torque, resulting in a spin relaxation.

Equivalence of spin Hall effect and spin-vorticity coupling, Eq. (1), pointed out in Ref. [18] provides an alternative view for the spin Hall-induced spin-orbit torque in bilayers of a ferromagnet and a nonmagnetic metal (NM) [29] (Fig. 1). A conventional picture explains the torque as a result of spin current generation in NM, which generates the spin accumulation at the interface [Fig. 1(a)]. In view of spin-vorticity coupling, the torque is due to the spin accumulation driven directly by electron vorticity near the interface formed as a result of a gradient of current [Fig. 1(b)]. As pointed out in Ref. [18], these pictures are physically equivalent.

For theoretical estimation of spin-orbit torque at interfaces, calculation of current-induced spin density has been employed phenomenological [31] and the first-principles [32] calculations. In Ref. [32], the response function of electron spin density to the applied current was calculated numerically for the case of Co/Pt and Mn/W interfaces, but the role of vorticity was not mentioned. The spin-vorticity coupling, Eq. (1), corresponds to the long-wavelength limit (the first order of derivative expansion) of the response function of spin and current.

II. ANOMALOUS HALL FLUID

We first revisit electron transport in a ferromagnetic metal with a uniform magnetization, i.e., the anomalous Hall system, studied from the hydrodynamic viewpoint in Ref. [27]. In that paper, the electron momentum flux density was calculated diagrammatically in the presence of a uniform magnetization at the linear response to the applied electric field treated as nonuniform. It was shown that there is a contribution to the viscosity coefficient arising from a coupling between the magnetization and vorticity of electron velocity, i.e., the magnetization-vorticity coupling. In terms of applied field $\boldsymbol{E}$, the coupling potential is $-\tilde{\zeta}_M^{\mathrm{f}}\boldsymbol{M}\cdot\boldsymbol{\omega}$, where $\boldsymbol{M}$ is the magnetization vector and $\boldsymbol{\omega}\equiv\nabla\times\boldsymbol{E}$ is a vorticity of the applied field and $\tilde{\zeta}_M^{\mathrm{f}}$ is a coefficient. The force density due to the coupling is

$$\boldsymbol{f}_{M\omega}=\tilde{\zeta}_M^{\mathrm{f}}\nabla(\boldsymbol{M}\cdot\boldsymbol{\omega}). \tag{2}$$

Such a coupling, regarded as a limit of spin-vorticity coupling where spin has a finite expectation value, has been argued from phenomenological grounds [15] and derived microscopically [27]. It is consistent with the Hall viscosity under a uniform external magnetic field studied in Ref. [21].

Here we present a phenomenological argument to derive the magnetization-vorticity coupling taking account of the anomalous Hall effect in the conventional fluid theory [33,34]. Fluid dynamics is described by the momentum flux density, π_{ij}, which is an expectation value $\langle\hat{p}_i\hat{v}_j\rangle$ of momentum and velocity operators, $\hat{p}$ and $\hat{v}$, respectively (i, j are spatial directions). Its divergence is the force density for the fluid, $f_i=-\nabla_j\pi_{ij}$. In nonmagnetic fluids with high symmetry, π_{ij} is written in terms of current density $\boldsymbol{j}$ as $\pi_{ij}=\zeta_0\delta_{ij}(\nabla\cdot\boldsymbol{j})+\eta_0[\nabla_i j_j+\nabla_j j_i]$, where ζ_0 and η_0 are viscosity constants [33]. The momentum flux density may have an antisymmetric component, π_{ij}^{a}, which is written generally as $\pi_{ij}^{\mathrm{a}}=\epsilon_{ijk}a_k$, where $\boldsymbol{a}$ is a vector invariant by the parity inversion ($\boldsymbol{r}\to-\boldsymbol{r}$). Without broken symmetry, vorticity $\boldsymbol{\omega}_{\mathrm{e}}(=\nabla\times\boldsymbol{j})$ is allowed as vector $\boldsymbol{a}$, resulting in an antisymmetric component $\pi_{ij}^{\mathrm{a}}=\frac{\xi_0}{2}(\nabla_i j_j-\nabla_j j_i)$ with a constant ξ_0 [34]. The electron current density is proportional to the applied field as $\boldsymbol{j}=\sigma_{\mathrm{e}}\boldsymbol{E}$, where σ_{e} is the diagonal conductivity in the case of high symmetry. The momentum flux density in this case is therefore [33,34]

$$\pi_{ij}=\zeta\delta_{ij}(\nabla\cdot\boldsymbol{E})+\eta[\nabla_i E_j+\nabla_j E_i]+\epsilon_{ijk}a_k, \tag{3}$$

with $\zeta\equiv\zeta_0\sigma_{\mathrm{e}}$ and $\eta\equiv\eta_0\sigma_{\mathrm{e}}$ and $\boldsymbol{a}=\xi\boldsymbol{\omega}$ ($\xi\equiv\xi_0\sigma_{\mathrm{e}}$).

In the presence of magnetization, the anomalous Hall effect tends to distort electron motion toward a perpendicular direction, i.e., $\boldsymbol{j}$ is modified to be $\boldsymbol{j}+\alpha_M(\hat{\boldsymbol{M}}\times\boldsymbol{j})$, where α_M is a constant and $\hat{\boldsymbol{M}}\equiv\boldsymbol{M}/|M|$. This means that anomalous Hall fluid has another driving field $\hat{\boldsymbol{M}}\times\boldsymbol{E}$ besides the electric field, which is a vector called a troidal moment:

$$\hat{\boldsymbol{M}}\times\boldsymbol{E}\equiv\boldsymbol{T}_{\hat{\boldsymbol{M}}}. \tag{4}$$

The troidal moment induces new components of the momentum flux density,

$$\pi_{ij}^M=\zeta_M\delta_{ij}(\nabla\cdot\boldsymbol{T}_{\hat{\boldsymbol{M}}})+\eta_M[\nabla_i T_{\hat{\boldsymbol{M}},j}+\nabla_j T_{\hat{\boldsymbol{M}},i}]+\epsilon_{ijk}a_{M,k}, \tag{5}$$

in the same manner as an electric field [Eq. (3)]. A possible vector $\boldsymbol{a}_M$ in the anomalous Hall fluid is [27]

$$\boldsymbol{a}_M=\xi_M^{\omega}(\hat{\boldsymbol{M}}\times\boldsymbol{\omega})+\xi_M^{\mathrm{v}}\hat{\boldsymbol{M}}(\nabla\cdot\boldsymbol{E})+\xi_M^{T}(\nabla\times\boldsymbol{T}_{\hat{\boldsymbol{M}}}), \tag{6}$$

where ξ_M^{ω}, ξ_M^{v}, and ξ_M^{T} are coefficients representing the anomalous Hall component of vorticity, volume change, and troidal moment, respectively. In the microscopic calculation in the ohmic regime in Ref. [27], ξ_M^{ω} and ξ_M^{v} arise from the side-jump process, while ξ_M^{T} vanishes. Using $\nabla\times\boldsymbol{T}_{\hat{\boldsymbol{M}}}=\hat{\boldsymbol{M}}(\nabla\cdot\boldsymbol{E})-(\hat{\boldsymbol{M}}\cdot\nabla)\boldsymbol{E}$ for the present case of uniform $\hat{\boldsymbol{M}}$, different representations of $\boldsymbol{a}_M$ are possible. In metals, $\nabla\cdot\boldsymbol{E}=0$, and $\nabla\times\boldsymbol{T}_{\hat{\boldsymbol{M}}}=-(\hat{\boldsymbol{M}}\cdot\nabla)\boldsymbol{E}$, resulting in $\boldsymbol{a}_M=\xi_M^{\omega}\nabla(\hat{\boldsymbol{M}}\cdot\boldsymbol{E})+\tilde{\xi}_M^{T}(\nabla\times\boldsymbol{T}_{\hat{\boldsymbol{M}}})$, where $\tilde{\xi}_M^{T}\equiv\xi_M^{T}+\xi_M^{\omega}$. The first term ξ_M^{ω} has no physical effect because its force density vanishes ($\nabla\times\nabla=0$) and is neglected. The antisymmetric component is therefore written simply as a rotation of the troidal moment,

$$\boldsymbol{a}_M=\tilde{\xi}_M^{T}(\nabla\times\boldsymbol{T}_{\hat{\boldsymbol{M}}}), \tag{7}$$

in the same manner as Eq. (3) for the electric field. The force density calculated from Eq. (5) in metal thus reads

$$f_{M,i}\equiv-\nabla_j\pi_{ij}^M=-\zeta_M^f\nabla_i(\nabla\cdot\boldsymbol{T}_{\hat{\boldsymbol{M}}})-\eta_M^f\nabla^2 T_{\hat{\boldsymbol{M}},i} \tag{8}$$

where $\zeta_M^f\equiv\zeta_M+\eta_M+\tilde{\xi}_M^T$, $\eta_M^f\equiv\eta_M-\tilde{\xi}_M^T$. The result is consistent with that obtained without using $\boldsymbol{T}_{\hat{\boldsymbol{M}}}$ in Ref. [27]. In the case of uniform magnetization, the divergence of a troidal moment is the magnetization-vorticity coupling:

$$\nabla\cdot\boldsymbol{T}_{\hat{\boldsymbol{M}}}=-(\hat{\boldsymbol{M}}\cdot\boldsymbol{\omega}). \tag{9}$$

Furthermore, using $\nabla^2\boldsymbol{T}_{\hat{\boldsymbol{M}}}=-\nabla(\hat{\boldsymbol{M}}\cdot\boldsymbol{\omega})+(\hat{\boldsymbol{M}}\cdot\nabla)\boldsymbol{\omega}$, the force density is written in terms of vorticity as

$$\boldsymbol{f}_M=\tilde{\zeta}_M^f\nabla(\hat{\boldsymbol{M}}\cdot\boldsymbol{\omega})+\tilde{\xi}_M^{\omega}(\hat{\boldsymbol{M}}\cdot\nabla)\boldsymbol{\omega}, \tag{10}$$

where $\tilde{\zeta}_M^f\equiv\zeta_M^f+\eta_M^f$ and $\tilde{\xi}_M^{\omega}\equiv\xi_M^{\omega}-\eta_M^f$. The first term on the right-hand side of Eq. (10) is a conservative force arising from the magnetization-vorticity coupling, while the second term is a nonconservative force, $\tilde{\xi}_M^{\omega}[\nabla\times(\boldsymbol{\omega}\times\hat{\boldsymbol{M}})]$. Equation (10) was derived by a microscopic calculation in Ref. [27], although the troidal moment explanation was not provided there. The two contributions, conservative and nonconservative, to the vorticity-induced motive force leads to an anisotropic motive force with respect to the direction of $\hat{\boldsymbol{M}}$ (see Sec. III A).

III. SPIN-RESOLVED MOMENTUM FLUX DENSITY AND SPIN MOTIVE FORCE

In this section, we consider the spin transport, i.e., the spin-resolved hydrodynamic equation for electrons, in ferromagnets. Although the method employed is different, the study here is essentially an extension of Refs. [11,27] to a ferromagnetic spinful case. The momentum flux density is defined spin dependent as $\pi_{ij}^{s,\alpha}\equiv\langle\hat{p}_i\hat{v}_j\sigma_\alpha\rangle$, where σ_α is the Pauli matrix (α denotes spin direction). The time derivative of the spin-resolved momentum density

$$p_i^{\alpha}\equiv\langle\hat{p}_i\sigma_\alpha\rangle \tag{11}$$

is represented in terms of $\pi_{ij}^{s,\alpha}$ as

$$\dot{p}_i^{\alpha}=-\nabla_j\pi_{ij}^{s,\alpha}. \tag{12}$$

We introduce a unit vector $\hat{\boldsymbol{s}}$ to represent the spin direction as

$$\boldsymbol{\pi}_{ij}^{s}\equiv\left(\pi_{ij}^{s,x},\pi_{ij}^{s,y},\pi_{ij}^{s,z}\right)\equiv\hat{\boldsymbol{s}}\overline{\pi}_{ij}^{s}, \tag{13}$$

where $\overline{\pi}_{ij}^{s}\equiv[(\pi_{ij}^{s,x})^2+(\pi_{ij}^{s,y})^2+(\pi_{ij}^{s,z})^2]^{1/2}$.

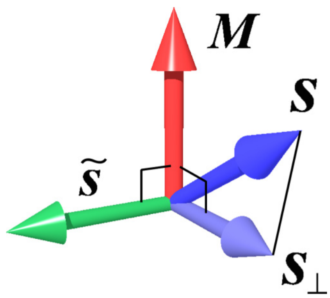

FIG. 2. Parameterization of spin vectors, $\boldsymbol{s}_\perp \equiv \boldsymbol{s} - \hat{\boldsymbol{M}}(\hat{\boldsymbol{M}}\cdot\boldsymbol{s})$ and $\tilde{\boldsymbol{s}} \equiv \boldsymbol{s}\times\hat{\boldsymbol{M}}$.

The effect of spin (called the internal angular momentum in Ref. [15]) on the electron fluid was theoretically discussed on a symmetry basis in Ref. [15], where possible contributions of the total (spin-neutral) momentum flux density when spin is present were argued.

Here we represent the momentum flux density as spin polarized, introducing a spin direction $\hat{\boldsymbol{s}}$. The spatial derivative of the spin-resolved momentum flux density represents a force acting on spin polarization, i.e., the spin motive force [35]. The spin motive force is a convenient quantity to discuss spin current generation.

One needs, however, to understand that spin-resolved quantities p_i^α and $\boldsymbol{\pi}_{ij}^s$ are not directly measurable and are not physical observables. This is because the flux density $\boldsymbol{\pi}_{ij}^s$ is not conserved and cannot be defined uniquely, as is in the case of spin current [36]. In fact, $\pi_{ij}^{s,\alpha}$ is an expectation value of $\langle \hat{p}_i \hat{v}_j \sigma_\alpha\rangle$, i.e., the velocity ($\hat{v}$) of momentum and spin [see Eqs. (29) and (30)], while its expression depends on the ordering of the three operators $\hat{p}_i$, $\hat{v}_j$, and σ_α that are noncommutative and is thus not unique. Like in the case of spin Hall effect, predictions for experiments need to be provided in terms of physical spin accumulation or charge current by solving the hydrodynamic Eq. (12). Here in this paper, we discuss spin-resolved momentum flux density and spin motive force for understanding roles of vorticity on the spin transport and leave explicit calculations of hydrodynamic equations as future work. Spin density calculation is carried out independently from the momentum flux density analysis in Sec. IV.

A. Phenomenological argument

Let us first proceed phenomenologically, extending the argument in Sec. II. We first focus on the symmetric (s) component, $\boldsymbol{\pi}_{ij}^{s(\mathrm{s})}$. Based on the expression for the anomalous Hall system [27] [Eq. (5)], we expect an adiabatic component having a spin polarization $\hat{\boldsymbol{s}}$ along the magnetization as ($\eta_s^\parallel$ and $\zeta_s^\parallel$ are coefficients)

$$\overline{\pi}_{ij}^{s(\mathrm{s})\parallel} = (\hat{\boldsymbol{s}}\cdot\hat{\boldsymbol{M}})\big(\zeta_s^\parallel(\hat{\boldsymbol{M}}\cdot\boldsymbol{\omega})\delta_{ij} + \eta_s^\parallel(\nabla_i T_{\hat{\boldsymbol{M}},j} + \nabla_j T_{\hat{\boldsymbol{M}},i})\big). \quad (14)$$

As for the nonadiabatic contribution due to perpendicular spin polarization, we introduce (Fig. 2)

$$\hat{\boldsymbol{s}}_\perp \equiv \hat{\boldsymbol{s}} - \hat{\boldsymbol{M}}(\hat{\boldsymbol{M}}\cdot\hat{\boldsymbol{s}}), \quad (15)$$

whose contribution is

$$\overline{\pi}_{ij}^{s(\mathrm{s})\perp} = \zeta_s^\perp(\hat{\boldsymbol{s}}_\perp\cdot\boldsymbol{\omega})\delta_{ij} + \eta_s^\perp(\nabla_i T_{\hat{\boldsymbol{s}}_\perp,j} + \nabla_j T_{\hat{\boldsymbol{s}}_\perp,i}), \quad (16)$$

where

$$\boldsymbol{T}_{\hat{\boldsymbol{s}}_\perp} \equiv \hat{\boldsymbol{s}}_\perp \times \boldsymbol{E} \quad (17)$$

is a troidal moment due to the spin polarization. Another spin polarization perpendicular to $\hat{\boldsymbol{M}}$ is

$$\tilde{\boldsymbol{s}} \equiv \hat{\boldsymbol{s}} \times \hat{\boldsymbol{M}}, \quad (18)$$

which is induced by an anomalous Hall effect in the direction perpendicular to $\boldsymbol{M}$, and its contribution reads

$$\overline{\pi}_{ij}^{s(\mathrm{s})\perp'} = \zeta_s^{\perp'}(\tilde{\boldsymbol{s}}\cdot\boldsymbol{\omega})\delta_{ij} + \eta_s^{\perp'}(\nabla_i T_{\tilde{\boldsymbol{s}},j} + \nabla_j T_{\tilde{\boldsymbol{s}},i}), \quad (19)$$

where

$$\boldsymbol{T}_{\tilde{\boldsymbol{s}}} \equiv \tilde{\boldsymbol{s}} \times \boldsymbol{E} \quad (20)$$

and $\zeta_s^{\perp'}$ and $\eta_s^{\perp'}$ are constants.

Antisymmetric contributions with spin direction α, $\pi_{ij}^{s,\alpha} \equiv \epsilon_{ijk} a_k^{s,\alpha}$, are similarly argued. We consider the case of $\nabla\cdot\boldsymbol{E} = 0$. As we saw in Eq. (7), only the troidal moment contribution survives in this case. Besides the adiabatic component proportional to Eq. (7), we therefore have (with coefficients $\xi_s^{T_{\hat{s}}}$ and $\xi_s^{T_{\tilde{s}}}$)

$$a_k^{s,\alpha} = \xi_s^{T_{\hat{s}}}(\nabla\times\boldsymbol{T}_{\hat{\boldsymbol{s}}}) + \xi_s^{T_{\tilde{s}}}(\nabla\times\boldsymbol{T}_{\tilde{\boldsymbol{s}}}). \quad (21)$$

(Here coefficients are defined using $\hat{\boldsymbol{s}}$ instead of $\hat{\boldsymbol{s}}_\perp$, i.e., neglecting the adiabatic component.)

Due to Eq. (12), a spin-resolved force (a spin motive force) acting on the electron spin polarized along direction α is

$$f_{s,i}^\alpha \equiv -\nabla_j \pi_{ij}^{s,\alpha} \equiv \hat{\boldsymbol{s}}\overline{f}_{s,i}. \quad (22)$$

As seen in Eq. (10) for the case of anomalous Hall fluid, the motive force when $\nabla\cdot\boldsymbol{E} = 0$ is written in terms of vorticity. The adiabatic contribution parallel to $\hat{\boldsymbol{M}}$ is essentially the same as the anomalous Hall case [Eq. (10)], i.e.,

$$\overline{\boldsymbol{f}}_s^\parallel = (\hat{\boldsymbol{s}}\cdot\hat{\boldsymbol{M}})\big[\tilde{\zeta}_s^{f,\parallel}\nabla(\hat{\boldsymbol{M}}\cdot\boldsymbol{\omega}) + \tilde{\xi}_s^{\omega,\parallel}(\hat{\boldsymbol{M}}\cdot\nabla)\boldsymbol{\omega}\big], \quad (23)$$

with constants $\tilde{\zeta}_s^{f,\parallel}$ and $\tilde{\xi}_s^{\omega,\parallel}$, while other contributions lead to motive force depending on the spin polarization as

$$\overline{\boldsymbol{f}}_s^\perp = \tilde{\zeta}_s^{f,\perp}\nabla(\hat{\boldsymbol{s}}\cdot\boldsymbol{\omega}) + \tilde{\xi}_s^{\omega,\perp}(\hat{\boldsymbol{s}}\cdot\nabla)\boldsymbol{\omega} + \tilde{\zeta}_s^{f,\perp'}\nabla(\tilde{\boldsymbol{s}}\cdot\boldsymbol{\omega}) + \tilde{\xi}_s^{\omega,\perp'}(\tilde{\boldsymbol{s}}\cdot\nabla)\boldsymbol{\omega}. \quad (24)$$

The contributions represented by coefficients $\tilde{\zeta}_s^{f,\perp}$ and $\tilde{\zeta}_s^{f,\perp'}$ are conservative forces due to coupling potential to vorticity, while $\tilde{\xi}_s^{\omega,\perp}$ and $\tilde{\xi}_s^{\omega,\perp'}$ represent nonconservative forces. Interestingly, conservative forces induce spin polarization ($\hat{\boldsymbol{s}}$ or $\tilde{\boldsymbol{s}}$) along $\boldsymbol{\omega}$ and force along the gradient of $\boldsymbol{\omega}$, while the noncoservative ones induce force and spin in the direction of $\boldsymbol{\omega}$ and the gradient of $\boldsymbol{\omega}$, respectively.

Let us consider electron fluid in a thin film as in Fig. 3 and see the contributions of $\tilde{\zeta}_s^{f,\perp}$ and $\tilde{\xi}_s^{\omega,\perp}$ connecting vorticity and $\hat{\boldsymbol{s}}$. The driving field $\boldsymbol{E}$ includes all the forces acting on the electrons, such as friction force from the boundary, besides the applied external electric field. The field $\boldsymbol{E}$ is therefore locally proportional to the local fluid current $\boldsymbol{j}$ neglecting the higher order contributions of the spin-orbit interaction, and is suppressed near the boundary as in Fig. 3 [27]. This suppression of fluid velocity in the z direction leads to a vorticity along the y direction, $\omega_y = \partial_z E_x$. The vorticity changes signs on the

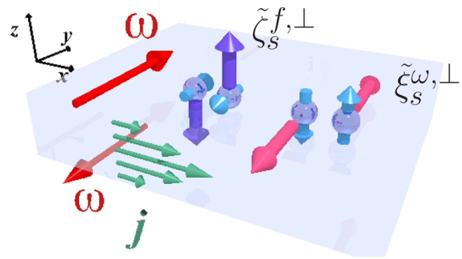

FIG. 3. A schematic picture showing spin motive forces of Eq. (24) in a thin film in the xy plane with applied current along the x direction. The contributions $\tilde{\zeta}_s^{f,\perp}$ and $\tilde{\xi}_s^{\omega,\perp}$ connecting vorticity and $\hat{\boldsymbol{s}}$ are depicted. At the boundaries, the flow vanishes, meaning that total effective field $\boldsymbol{E}$ including the applied field and friction force from the boundary vanishes due to proportionality of $\boldsymbol{j}$ and $\boldsymbol{E}$. The derivative $\partial_z E_x$ is therefore finite, namely, vorticity ω emerges near the boundary along the y direction. The vorticity has opposite signs on the upper and lower planes, resulting in $\partial_z \omega_y$. The contribution of conventional conservative spin-vorticity coupling, the term $\tilde{\zeta}_s^{f,\perp}$, thus induces a spin polarization (short arrows with sphere) along the y direction, and motive force along the z axis (blue arrows). The nonconservative contribution, $\tilde{\xi}_s^{\omega,\perp}$, in contrast, induces a spin polarization along the z direction, and motive force along the y axis (magenta arrows).

upper and lower boundaries and changes along the z direction. For electron spin along $+y$ direction, the conservative spin motive force is along the z axis as $f_z^{\zeta} = \tilde{\zeta}_s^{f,\perp} \nabla_z \boldsymbol{\omega}_y$, i.e., is in the $-z$ direction (if $\tilde{\zeta}_s^{f,\perp} > 0$), while it is $+z$ direction for the electron spin pointing in the $-y$ direction. Thus spin current along the z axis is induced by the spin-vorticity coupling as argued in previous works [9]. The nonconservative motive force described by the term $\tilde{\xi}_s^{\omega,\perp}$, which is mainly from the asymmetric viscosity, acts in the $-y$ $(+y)$ direction for spin polarization along $+z$ $(-z)$ direction, inducing a spin current in the y direction (Fig. 3). The contribution $\tilde{\zeta}_s^{f,\perp'}$ and $\tilde{\xi}_s^{\omega,\perp'}$ induce orthogonal spin polarizations to $\tilde{\zeta}_s^{f,\perp}$ and $\tilde{\xi}_s^{\omega,\perp}$, respectively. The adiabatic contributions and anomalous Hall contributions are discussed by replacing $\hat{\boldsymbol{s}}$ by $\hat{\boldsymbol{M}}$ in the above argument.

In the next section, we carry out microscopic calculations on a simplified model to confirm the above argument.

B. Microscopic derivation

We first derive the definition of the spin-resolved momentum flux density by deriving a hydrodynamic equation for the time-derivative of momentum density, $\dot{\boldsymbol{p}}$, following Refs. [26,27]. In the present case with spin, spin-resolved momentum density, defined as

$$p_i^{\alpha} \equiv \langle c^{\dagger} \hat{p}_i \sigma_{\alpha} c \rangle, \tag{25}$$

is considered, where $\hat{p}_i$ and σ_α denote the operators for momentum and spin (i and α represents direction), respectively, $\langle\rangle$ denotes quantum average, and c and $c^\dagger$ are electron field operators. Its time derivative is derived by use of the Heisenberg equation of motion, $\dot{p}_i^{\alpha} = i\langle [H, c^{\dagger}\hat{p}_i\sigma_\alpha c]\rangle$, where $[A, B] \equiv AB - BA$ is a commutator and H is the total Hamiltonian. The Hamiltonian we consider is

$$H = \int d^3 r c^{\dagger} \left(\frac{-\nabla^2}{2m} - (\boldsymbol{M}\cdot\boldsymbol{\sigma}) \right) c + H_{\mathrm{so}} + H_{\mathrm{i}}, \tag{26}$$

where $\boldsymbol{M}$ is a vector representing the magnetization including the exchange coupling constant. The spin-orbit interaction by impurities is represented by

$$\begin{aligned} H_{\mathrm{so}} &= \lambda \int d^3 r c^{\dagger}(\boldsymbol{r})[(\nabla v(\boldsymbol{r}) \times \hat{\boldsymbol{p}})\cdot\boldsymbol{\sigma}] c(\boldsymbol{r}) \\ &= i\lambda \sum_{\boldsymbol{k}\boldsymbol{k}'} v_{\boldsymbol{k}'-\boldsymbol{k}} (\boldsymbol{k}' \times \boldsymbol{k}) \cdot c_{\boldsymbol{k}'}^{\dagger} \boldsymbol{\sigma} c_{\boldsymbol{k}}, \end{aligned} \tag{27}$$

where λ is a coupling constant, $v(\boldsymbol{r}) = v_{\mathrm{i}} \sum_{\boldsymbol{R}_n} \delta(\boldsymbol{r} - \boldsymbol{R}_n)$ is an impurity potential, where v_{i} and $\boldsymbol{R}_n$ are the strength of the impurity potential and the position of nth impurity, respectively, and the impurity scattering potential is $H_{\mathrm{i}} = \int d^3 r v(\boldsymbol{r}) c^{\dagger}(\boldsymbol{r}) c(\boldsymbol{r})$. The impurity scattering induces an electron lifetime of elastic scattering, τ, given by $\tau^{-1} = 2\pi \nu n_{\mathrm{i}} {v_{\mathrm{i}}}^2$, where n_{i} is the impurity concentration and ν is the density of states of electron. In this paper, we treat τ as spin-independent for simplicity.

A driving electric field for electron flow, $\boldsymbol{E}$, is included using a vector potential $\boldsymbol{A}$ satisfying $\boldsymbol{E} = -\dot{\boldsymbol{A}}$ [37]. As is known generally for transport theories, dominant nonequilibrium contributions for the case of time-independent $\boldsymbol{E}$ are those containing both retarded and advanced Green's functions [26], and we shall focus on these contributions. Spatial inhomogeneity is taken into account by expanding response functions with respect to the wave vector $\boldsymbol{q}$ of $\boldsymbol{E}$ to the linear order.

In the present model, the driving field is not only the applied external field but is an effective one that includes other extrinsic forces such as those introduced by boundaries. At the boundary, fluid velocity vanishes and this fact is imposed usually as a boundary condition in solving fluid dynamics. (See Ref. [24] for boundary effects.) In the present microscopic modeling of the ohmic fluid, such boundary effects are effectively taken into account by assuming that the total driving field vanishes at the boundary, as was done in Refs. [26,27]. This is because vanishing fluid velocity indicates that the force due to the applied field and the friction from the boundary cancel each other. Practically speaking, our total effective field is related to the actual current density $\boldsymbol{j}$, which vanishes at the boundary, via a local relation $\boldsymbol{E} = (\sigma_{\mathrm{e}})^{-1}\boldsymbol{j}$, where σ_{e} is a conductivity tensor. In the present analysis focusing on the lowest order of the spin-orbit interaction, σ_{e} can be treated as diagonal. (It would be an interesting future work to numerically solve the whole hydrodynamic equation, taking account of off-diagonal conductivity.)

The hydrodynamic equation for spin-resolved momentum density is (see Sec. A for derivation)

$$\dot{p}_i^{\alpha} = -\nabla_j \pi_{ij}^{s,\alpha} + f_{s,i}^{\alpha}, \tag{28}$$

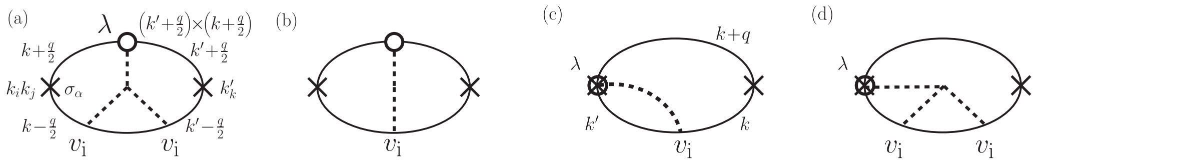

FIG. 4. Feynman diagrams for the dominant contribution to the spin-resolved momentum flux density $\pi^{s,\alpha}_{ijk}$ at the linear order in the spin-orbit interaction and linear response to the applied field, denoted by $\times$ at the right end (suffix k represents the direction of the applied field). Solid lines represent free electron Green's functions, where upper and lower lines denote retarded ($g^{\rm r}_{\boldsymbol{k}}$) and advanced ($g^{\rm a}_{\boldsymbol{k}}$) Green's functions, respectively, and $\boldsymbol{k}$ and $\boldsymbol{k}'$ are the electron wave vectors. The wave vector $\boldsymbol{q}$ is that of the external field and represents the inhomogeneity of flow. Complex conjugate processes (turned upside down) are also taken into account. (a) Skew-scattering contribution $\pi^{({\rm ss})\alpha}_{ijk}$. The left vertex with k_ik_j represents the vertex for the momentum flux density, and a vertex with λ denotes the spin-orbit interaction. (b) A small contribution that is neglected. (c) The contribution arising from the anomalous velocity δv in $\pi^{0\alpha}_{ijk}$, called the side-jump contribution. (d) The anomalous contribution $\delta\pi^{\alpha}_{ijk}$.

where $\pi^{s,\alpha}_{ij} \equiv \pi^{0\alpha}_{ij} + \delta\pi^{\alpha}_{ij}$ with

$$\pi^{0\alpha}_{ij}(\boldsymbol{r},t) \equiv -i{\rm tr}[\hat{p}_i\{\hat{v}_j,\sigma_\alpha\}G^<(\boldsymbol{r},t,\boldsymbol{r},t)] \tag{29}$$

is a conventional contribution in the form of momentum and velocity (tr is a trace over spin and $\{A,B\} \equiv AB + BA$), while

$$\delta\pi^{\alpha}_{ij}(\boldsymbol{r},t) \equiv -i\frac{\lambda}{2}{\rm tr}[(\nabla_i\nabla_k V)(\delta_{j\alpha}\delta_{k\beta} - \delta_{j\beta}\delta_{k\alpha}) \times \sigma_\beta G^<(\boldsymbol{r},t,\boldsymbol{r},t)] \tag{30}$$

is an anomalous contribution from the spin-orbit potential. Here $G^<(\boldsymbol{r},t,\boldsymbol{r}',t) \equiv i\langle c^\dagger(\boldsymbol{r},t)c(\boldsymbol{r}',t')\rangle$ is the full lesser Green's function including the external field and

$$\hat{v}_j = \frac{\hat{p}_j}{m} + \delta\hat{v}_j \tag{31}$$

is the total velocity operator with the anomalous velocity

$$\delta\hat{v}_j = -\lambda(\nabla V \times \boldsymbol{\sigma})_j \tag{32}$$

due to the spin-orbit interaction. The term $f^{\alpha}_{s,i}$ in Eq. (28) is the one which cannot be written as a divergence of flow, interpreted purely as a force. The spin-resolved momentum, which is essentially the spin current, is not conserved in the presence of spin relaxation processes, and this is why we have force density besides the momentum flux density. This fact means that the definition of the spin-dependent momentum flux density is not unique. Nevertheless, it is a useful quantity to study the roles of vorticity on the spin transport, like spin motive force (spin gauge field) in spintronics [38].

Based on the above Hamiltonian, we calculate the momentum flux density, Eqs. (29) and (30), as the linear response to an external field $\boldsymbol{E}$. The momentum flux density is written as $\pi^{s,\alpha}_{ij} = \pi^{s,\alpha}_{ijk}E_k$, where $\pi^{s,\alpha}_{ijk}$ is a correlation function of spin momentum current and current calculated diagrammatically (Fig. 4) using the Green's function method [37] in the same manner as Refs. [26,27]. The spin-orbit interaction, which is essential to couple electron flow and its spin, is included to the linear order. There are two spin-orbit processes, one arising from the normal velocity $\frac{\boldsymbol{p}}{m}$, the contribution historically called skew scattering contribution, and the other arising from the anomalous velocity $\delta\boldsymbol{v}$, called the side-jump contribution. Below, we evaluate dominant contributions to $\pi^{s,\alpha}_{ijk}$, which are those including both retarded and advanced Green's functions, following Refs. [26,27].

1. Skew-scattering contribution

We first consider the process of Fig. 4(a) (skew scattering), which is

$$\pi^{({\rm ss})\alpha}_{ijk}(\boldsymbol{q}) = \frac{e}{V^3}\frac{i}{\pi}\frac{\lambda n_{\rm i}{v_{\rm i}}^3}{m^2}{\rm Re}\sum_{\boldsymbol{k}\boldsymbol{k}'}k_ik_jk'_k\left[\left(\boldsymbol{k}'+\frac{\boldsymbol{q}}{2}\right)\times\left(\boldsymbol{k}+\frac{\boldsymbol{q}}{2}\right)\right]_\beta \times {\rm tr}\left[\sigma_\alpha g^{\rm r}_{\boldsymbol{k}+\frac{\boldsymbol{q}}{2}}\sigma_\beta g^{\rm r}_{\boldsymbol{k}'+\frac{\boldsymbol{q}}{2}}g^{\rm a}_{\boldsymbol{k}'-\frac{\boldsymbol{q}}{2}}g^{\rm a}_{\boldsymbol{k}''}g^{\rm a}_{\boldsymbol{k}-\frac{\boldsymbol{q}}{2}}\right], \tag{33}$$

where $\boldsymbol{q}$ is the wave vector of the external field, $g^{\rm r}_{\boldsymbol{k}} \equiv [-\frac{k^2}{2m} + \epsilon_F + \boldsymbol{M}\cdot\boldsymbol{\sigma} + \frac{i}{2\tau}]^{-1}$ is the free electron retarded green's function with elastic lifetime τ arising from the impurities and $g^{\rm a}_{\boldsymbol{k}} \equiv (g^{\rm r}_{\boldsymbol{k}})^*$, ϵ_F being the Fermi energy. The real (imaginary) part is denoted by Re (Im).

We calculate the response function to the lowest order in the external wave vector $\boldsymbol{q}$ and neglecting contributions smaller by a factor of $(\epsilon_F\tau)^{-1}$. Noting that

$${\rm tr}[\sigma^\alpha A\sigma^\beta B] = (\delta_{\alpha\beta} - \delta_{\alpha z}\delta_{\beta z})\sum_\sigma A_\sigma B_{-\sigma} + \delta_{\alpha z}\delta_{\beta z}\sum_\sigma A_\sigma B_\sigma - i\epsilon_{\alpha\beta z}\sum_\sigma \sigma A_\sigma B_{-\sigma} \tag{34}$$

for diagonal matrices $A = \begin{pmatrix} A_+ & 0 \\ 0 & A_- \end{pmatrix}$ and B, the trace over the spin is calculated to obtain [neglecting $O(q^2)$]

$$\pi^{({\rm ss})\alpha}_{ijk}(\boldsymbol{q}) = i\sum_\sigma {\rm Re}\left[I^{-\sigma,\sigma}_{ijk\alpha} + \delta_{\alpha z}\left(I^{\sigma,\sigma}_{ijkz} - I^{-\sigma,\sigma}_{ijkz}\right) + i\epsilon_{\alpha\beta z}\sigma I^{-\sigma,\sigma}_{ijk\beta}\right], \tag{35}$$

where $I^{\sigma'\sigma}_{ijk\alpha} \equiv \frac{1}{\pi}\frac{\lambda n_{\rm i}{v_{\rm i}}^3}{m^2}\tilde{I}^{\sigma'\sigma}_{ijk\alpha}$, with

$$\tilde{I}^{\sigma'\sigma}_{ijk\alpha} = \frac{1}{V^3}\sum_{\boldsymbol{k}\boldsymbol{k}'\boldsymbol{k}''}k_ik_jk'_k(\boldsymbol{k}'\times\boldsymbol{k})_\alpha g^{\rm r}_{\boldsymbol{k}+\frac{\boldsymbol{q}}{2},\sigma'}g^{\rm r}_{\boldsymbol{k}'+\frac{\boldsymbol{q}}{2},\sigma}g^{\rm a}_{\boldsymbol{k}'-\frac{\boldsymbol{q}}{2},\sigma}g^{\rm a}_{\boldsymbol{k}'',\sigma} \times g^{\rm a}_{\boldsymbol{k}-\frac{\boldsymbol{q}}{2},\sigma}. \tag{36}$$

The summation over the wave vectors are carried out using

$$\frac{1}{V}\sum_{\boldsymbol{k}} g^{\mathrm{a}}_{\boldsymbol{k},\sigma} = i\pi\nu_\sigma, \quad \frac{1}{V}\sum_{\boldsymbol{k}} k_i k_j g^{\mathrm{r}}_{\boldsymbol{k},\sigma} g^{\mathrm{a}}_{\boldsymbol{k},\sigma} = \frac{2\pi}{3}\nu_\sigma k_{F\sigma}^2 \tau\delta_{ij},$$

$$\frac{1}{V}\sum_{\boldsymbol{k}} k_i k_j k_k g^{\mathrm{r}}_{\boldsymbol{k}+\frac{\boldsymbol{q}}{2},\sigma} g^{\mathrm{a}}_{\boldsymbol{k}-\frac{\boldsymbol{q}}{2},\sigma'} = i\frac{\pi}{15m}(\delta_{ij}q_k + \delta_{ik}q_j + \delta_{jk}q_i)\frac{\nu_\sigma k_{F\sigma}^4 + \nu_{\sigma'}k_{F\sigma'}^4}{\left[(\sigma-\sigma')M + \frac{i}{\tau}\right]^2}, \tag{37}$$

where ν_σ, $k_{F\sigma}$ are density of states at the Fermi energy and Fermi wave vector of electron with spin $\sigma = \pm$, respectively, as

$$\tilde{I}^{\sigma'\sigma}_{ijk\alpha} = -\frac{2\pi^3}{45m}(\nu_\sigma)^2(k_{F\sigma})^2\tau\epsilon_{\alpha km}(\delta_{ij}q_m + \delta_{im}q_j + \delta_{jm}q_i)\frac{\nu_{\sigma'}k_{F\sigma'}^4 + \nu_\sigma k_{F\sigma}^4}{\left[(\sigma'-\sigma)M + \frac{i}{\tau}\right]^2}. \tag{38}$$

Thus,

$$\pi^{(\mathrm{ss})\alpha}_{ijk}(\boldsymbol{q}) = i\Bigg[[(\hat{\boldsymbol{\alpha}}\times\boldsymbol{q})_k\delta_{ij} + \epsilon_{ik\alpha}q_j + \epsilon_{jk\alpha}q_i]\mathrm{Re}\sum_\sigma J^\sigma_- + \delta_{\alpha z}[(\hat{\boldsymbol{z}}\times\boldsymbol{q})_k\delta_{ij} + \epsilon_{ikz}q_j + \epsilon_{jkz}q_i]\mathrm{Re}\sum_\sigma (J^\sigma_+ - J^\sigma_-)$$
$$- \epsilon_{\alpha\beta z}[-\epsilon_{\beta kl}q_l\delta_{ij} + \epsilon_{ik\beta}q_j + \epsilon_{jk\beta}q_i]\mathrm{Im}\sum_\sigma \sigma J^\sigma_-\Bigg], \tag{39}$$

where

$$J^\sigma_- = \frac{2\pi^2}{45m^3}\lambda n_{\mathrm{i}} v_{\mathrm{i}}{}^3\left(\sum_{\sigma'}\nu_{\sigma'}k_{F\sigma'}^4\right)(\nu_\sigma)^2(k_{F\sigma})^2\tau\frac{4M^2 - \frac{1}{\tau^2} + 4i\sigma\frac{M}{\tau}}{\left(4M^2 + \frac{1}{\tau^2}\right)^2},$$

$$J^\sigma_+ = -\frac{2\pi^2}{45m^3}\lambda n_{\mathrm{i}} v_{\mathrm{i}}{}^3(\nu_\sigma)^3(k_{F\sigma})^6 2\tau^3. \tag{40}$$

We thus obtain

$$\pi^{(\mathrm{ss})\alpha}_{ij} = \eta^{(\mathrm{ss})}_\parallel \hat{M}_\alpha\big((\hat{\boldsymbol{M}}\cdot\boldsymbol{\omega})\delta_{ij} + \nabla_i T_j + \nabla_j T_i\big)$$
$$+ \eta^{(\mathrm{ss})}_\perp\big((\hat{\boldsymbol{\alpha}}_\perp\cdot\boldsymbol{\omega})\delta_{ij} + \nabla_i T^{\alpha_\perp}_j + \nabla_j T^{\alpha_\perp}_i\big)$$
$$+ \eta^{(\mathrm{ss})}_{\perp'}\big((\hat{\boldsymbol{\alpha}}_{\perp'}\cdot\boldsymbol{\omega})\delta_{ij} + \nabla_i T^{\alpha_{\perp'}}_j + \nabla_j T^{\alpha_{\perp'}}_i\big), \tag{41}$$

where $\hat{\boldsymbol{\alpha}}$ is the unit vector along the spin direction α, $\hat{\boldsymbol{\alpha}}_\perp \equiv \hat{\boldsymbol{\alpha}} - \hat{\boldsymbol{M}}(\hat{\boldsymbol{M}}\cdot\hat{\boldsymbol{\alpha}})$, $\hat{\boldsymbol{\alpha}}_{\perp'} \equiv \hat{\boldsymbol{M}}\times\hat{\boldsymbol{\alpha}}$, and

$$\eta^{(\mathrm{ss})}_\parallel \equiv -\mathrm{Re}\sum_\sigma J^\sigma_+,$$

$$\eta^{(\mathrm{ss})}_\perp \equiv -\mathrm{Re}\sum_\sigma J^\sigma_-,$$

$$\eta^{(\mathrm{ss})}_{\perp'} \equiv -\mathrm{Im}\sum_\sigma \sigma J^\sigma_-. \tag{42}$$

In terms of spin polarization vector $\hat{\boldsymbol{s}}$ [Eq. (13)], the amplitude of the flux density is

$$\overline{\pi}^{(\mathrm{ss})}_{ij} = \eta^{(\mathrm{ss})}_\parallel(\hat{\boldsymbol{s}}\cdot\hat{\boldsymbol{M}})\big((\hat{\boldsymbol{M}}\cdot\boldsymbol{\omega})\delta_{ij} + \nabla_i T_{\hat{\boldsymbol{M}},j} + \nabla_j T_{\hat{\boldsymbol{M}},i}\big)$$
$$+ \eta^{(\mathrm{ss})}_\perp((\hat{\boldsymbol{s}}_\perp\cdot\boldsymbol{\omega})\delta_{ij} + \nabla_i T_{s_\perp,j} + \nabla_j T_{s_\perp,i})$$
$$+ \eta^{(\mathrm{ss})}_{\perp'}((\hat{\boldsymbol{s}}_{\perp'}\cdot\boldsymbol{\omega})\delta_{ij} + \nabla_i T_{s_{\perp'},j} + \nabla_j T_{s_{\perp'},i}), \tag{43}$$

a result consistent with the phenomenological argument in Sec. III A.

Let us estimate the magnitude of the coefficients. Our analysis in the ohmic regime (dirty metal) assumes $\epsilon_F\tau \gg 1$. We first consider a strong ferromagnet with $M\tau \gg 1$. We simplify $\nu_+ \sim \nu_- \sim 1/\epsilon_F$ and $k_{F\sigma} \sim k_F$ for order of magnitude estimate and neglect numerical factors. We then have

$$J^\sigma_+ \sim \frac{\epsilon_{\mathrm{so}}}{m}\tau^2, \quad J^\sigma_- \sim \frac{\epsilon_{\mathrm{so}}}{m}\frac{1}{M^2}\left(1 + i\sigma\frac{1}{M\tau}\right), \tag{44}$$

and thus

$$\eta^{(\mathrm{ss})}_\parallel \sim \frac{\epsilon_{\mathrm{so}}}{m}\tau^2, \quad \eta^{(\mathrm{ss})}_\perp \sim \frac{\epsilon_{\mathrm{so}}}{m}\frac{1}{M^2}, \quad \eta^{(\mathrm{ss})}_{\perp'} \sim \frac{\epsilon_{\mathrm{so}}}{m}\frac{1}{M^3\tau}, \tag{45}$$

where $\epsilon_{\mathrm{so}} \equiv \lambda v_{\mathrm{i}} k_F{}^2$ is the energy scale of the spin-orbit interaction, namely, the adiabatic component is the largest, while $\eta^{(\mathrm{ss})}_\perp$ contribution is dominant as a nonadiabatic contribution.

In the limit of $M = 0$, $J^\sigma_+ = J^\sigma_- \sim \frac{\epsilon_{\mathrm{so}}}{m}\tau^2$ and we have

$$\eta^{(\mathrm{ss})}_\parallel = \eta^{(\mathrm{ss})}_\perp \sim \frac{\epsilon_{\mathrm{so}}}{m}\tau^2, \quad \eta^{(\mathrm{ss})}_{\perp'} = 0, \tag{46}$$

which is natural from the rotational symmetry when $M = 0$.

There is a similar process with less impurity scattering, shown in Fig. 4(b). Compared to the contribution $\pi^{(\mathrm{ss})\alpha}_{ij}$, it is without a factor of $i\pi\nu v_{\mathrm{i}}$. Due to the extra factor of i, the imaginary and real parts are replaced, resulting in a vanishing contribution for $M = 0$ and a reduction factor of $(M\tau)^{-1}$ in the case of $M\tau \gg 1$. Considering a factor of $\nu v_{\mathrm{i}} \sim \sqrt{\nu\tau}$, the contribution vanishes ($M = 0$) or smaller by a factor of $(M\tau)^{-1/2}$. We thus neglect this process.

2. *Side jump and other contributions*

The contributions arising from the anomalous velocity $\delta\boldsymbol{v}$ [the side-jump contribution, depicted in Fig. 4(c)] is

$$\pi^{(\mathrm{sj})\alpha}_{ijk}(\boldsymbol{q}) = \frac{-i}{4\pi}\frac{1}{V^2}\frac{\lambda n_{\mathrm{i}} v_{\mathrm{i}}^2}{2m}\epsilon_{\alpha jl}\sum_{\boldsymbol{k}\boldsymbol{k}'}(k' + k + q)_i\left(k + \frac{q}{2}\right)_k$$
$$\times (k' - k)_l \mathrm{Retr}\big[g^{\mathrm{r}}_{\boldsymbol{k}'} g^{\mathrm{r}}_{\boldsymbol{k}} g^{\mathrm{a}}_{\boldsymbol{k}+\boldsymbol{q}}\big]. \tag{47}$$

It turns out to be

$$\pi^{(\mathrm{sj})\alpha}_{ijk}(\boldsymbol{q}) = i\eta^{(\mathrm{sj})}_0\left(\frac{2}{3}\epsilon_{\alpha ij}q_k + \delta_{ik}\epsilon_{\alpha jl}q_l + \epsilon_{\alpha jk}q_i\right), \tag{48}$$

where

$$\eta^{(\mathrm{sj})}_0 \equiv \frac{\pi}{15}\frac{\lambda n_{\mathrm{i}} v_{\mathrm{i}}^2}{m^2}\sum_\sigma (\nu_\sigma)^2 k_{\mathrm{F}\sigma}^4\tau^2. \tag{49}$$

Thus, neglecting the term that vanishes in the force, we obtain

$$\pi^{(\mathrm{sj})}_{ij} = \eta^{(\mathrm{sj}),T_{\hat{s}}}(\nabla_i T_{\hat{s},j} + \nabla_j T_{\hat{s},i}) + \epsilon_{ijk}a^{(\mathrm{sj})}_k, \tag{50}$$

where

$$\boldsymbol{a}^{(\mathrm{sj})} = \xi^{(\mathrm{sj}),\mathrm{v}}\hat{\boldsymbol{s}}(\nabla\cdot\boldsymbol{E}) + \xi^{(\mathrm{sj}),T_{\hat{s}}}(\nabla\times\boldsymbol{T}_{\hat{s}}), \tag{51}$$

with $\eta^{(\mathrm{sj}),T_{\hat{s}}} = -\frac{1}{2}\eta^{(\mathrm{sj})}_0$, $\xi^{(\mathrm{sj}),\mathrm{v}} = \frac{2}{3}\eta^{(\mathrm{sj})}_0$, $\xi^{(\mathrm{sj}),T_{\hat{s}}} = -\frac{1}{2}\eta^{(\mathrm{sj})}_0$. A unique feature of the side-jump contribution is that it does not vanish for $M = 0$, in contrast to the skew-scattering contribution. In the same order of estimate as in Eqs. (45), we have

$$\eta^{(\mathrm{sj})}_0 \sim \frac{\epsilon_{\mathrm{so}}}{m}\sqrt{\frac{\tau^3}{\epsilon_F}}. \tag{52}$$

The nonadiabatic contribution with spin polarized perpendicular to $\hat{\boldsymbol{M}}$ is therefore dominated by the side-jump contribution instead of skew-scattering contribution represented by $\eta^{(\mathrm{ss})}_\perp$ in the disordered metal with $M\tau \gg 1$.

Finally, the anomalous contribution to the momentum flux density is [Fig. 4(d)]

$$\delta\pi^\alpha_{ij}(\boldsymbol{q}) = \frac{(-i)^2}{2V^3}\frac{\lambda n_{\mathrm{i}} v_{\mathrm{i}}^3}{m}\sum_{\boldsymbol{k}\boldsymbol{k}'\boldsymbol{k}''}(k'-k)_i(k'-k)_l\left(k'+\frac{q}{2}\right)_k \times(\delta_{j\alpha}\delta_{l\beta} - \delta_{j\beta}\delta_{l\alpha})\mathrm{tr}\left[\sigma_\beta\left(g^{\mathrm{r}}_{\boldsymbol{k}}g^{\mathrm{r}}_{\boldsymbol{k}''} + g^{\mathrm{a}}_{\boldsymbol{k}}g^{\mathrm{a}}_{\boldsymbol{k}''}\right)g^{\mathrm{r}}_{\boldsymbol{k}'}g^{\mathrm{a}}_{\boldsymbol{k}'+\boldsymbol{q}}\right]. \tag{53}$$

After some calculation, we obtain

$$\delta\pi^\alpha_{ijk}(\boldsymbol{q}) = i\delta\pi\left(\frac{8}{3}(\delta_{iz}\delta_{j\alpha} - \delta_{i\alpha}\delta_{jz})q_k + \delta_{ik}(q_z\delta_{j\alpha} - q_\alpha\delta_{jz}) - (\delta_{jz}\delta_{k\alpha} - \delta_{j\alpha}\delta_{kz})q_i\right), \tag{54}$$

where

$$\delta\pi \equiv -\frac{2\pi^3}{15m^2}\lambda n_{\mathrm{i}} v_{\mathrm{i}}^3\tau^2\sum_\sigma \sigma\nu_\sigma^3 k_{F\sigma}^4. \tag{55}$$

Neglecting the unphysical contribution that vanishes in the force,

$$\overline{\delta\pi}_{ij} = \delta\eta_{T_{\perp'}}(\nabla_i T_{\tilde{s},j} + \nabla_j T_{\tilde{s},i}) + \epsilon_{ijk}\delta a^{\tilde{s}}_k, \tag{56}$$

where $\delta\eta_{T_{\perp'}} = \delta\pi$ and

$$\delta\boldsymbol{a}^{\tilde{s}} = \delta\xi^{\mathrm{v}}\tilde{\boldsymbol{s}}(\nabla\cdot\boldsymbol{E}) + \delta\xi^{T_{\tilde{s}}}(\nabla\times\boldsymbol{T}_{\tilde{s}}), \tag{57}$$

with $\delta\xi^{\mathrm{v}} = \frac{8}{3}\delta\pi$, $\delta\xi^{T_{\tilde{s}}} = \delta\pi$. The order of magnitude for $M\tau \gg 1$ is $\delta\pi \sim \frac{\epsilon_{\mathrm{so}}}{m}\frac{\tau}{\epsilon_F}$ and is smaller than the side-jump contribution but is larger than the skew-scattering nonadiabatic contribution.

In the limit of $M = 0$, the order of magnitudes of $\eta^{(\mathrm{sj})}_0$ and $\delta\pi$ are the same as in the $M\tau \gg 1$ case. Thus, these contributions are smaller than the skew-scattering contribution for $M = 0$, Eqs. (46). The side-jump contribution being smaller than the skew scattering one is due to the fact that the contribution involves less Green's functions than the skew scattering, resulting in smaller order of $\epsilon_F\tau(\gg 1)$ considering the fact that the peak magnitude of the Green's function is $\sim\tau$. When $M\tau \gg 1$, in contrast, the side-jump contribution dominates over the skew scattering as for the perpendicular spin polarization, as the Green's functions for the spin-flip processes are suppressed to be $\sim M^{-1}$, while the side-jump process contains a contribution without spin flip [Eq. (47)].

The phenomenological results in Sec. III A are therefore confirmed by microscopic calculations in this subsection and coefficients were determined by use of microscopic quantities.

IV. VORTICITY-INDUCED SPIN

Spin-resolved force density represents a force acting on spin components, namely, spin motive force driving spin current. Although it would be interesting to explore spin transport phenomena solving the hydrodynamic equation with spin, we leave it as a future work and study the result of the spin current generation, namely, the spin accumulation induced by the vorticity-induced spin motive forces.

Like spin current, spin-resolved force density is not a clear physical observable, as the force acting on electrons with a particular spin is not detectable. In contrast, the spin density which we are going to calculate here is a physical observable. In fact, spin Hall effect originally argued as a relation between the spin density and an applied electric field by Dyakonov and Perel [19] is free from the ambiguity of definition of spin current [18]. Here we discuss spin density taking account of inhomogeneous electric field to support physical consequence of spin hydrodynamic equations.

A. Spin Hall effect in the viewpoint of spin-vorticity coupling

As was pointed out [18], an inhomogeneous electric field applied to a metal with spin-orbit interaction induces a spin density as in Eq. (1). This relation, indicating that the spin Hall effect is a consequence of spin-vorticity coupling, is a representation of spin Hall effect written in terms of spin density instead of spin current. The spin accumulation given by Eq. (1) in fact represents the spin accumulation formed at the edges as a result of spin current generated by the applied electric field. The expression corresponds to the clean system where electron diffusion is not relevant and, in the disordered case, the expression is multiplied by a diffusion propagator [18] [see Eq. (65)]. The spin generation by the spin Hall effect has been argued mostly in the absence of magnetization, to discuss the pure spin current [20]. When a magnetization is present, spin polarization along the magnetization $\hat{\boldsymbol{M}}$ (the adiabatic component) and orthogonal components $\hat{\boldsymbol{M}}\times\boldsymbol{\omega}$ arise, and spin density is extended as

$$\boldsymbol{s}(\boldsymbol{r}) = \lambda_{\mathrm{sh}}\boldsymbol{\omega} + \lambda_\parallel\hat{\boldsymbol{M}}(\hat{\boldsymbol{M}}\cdot\boldsymbol{\omega}) + \lambda_\perp(\hat{\boldsymbol{M}}\times\boldsymbol{\omega}), \tag{58}$$

with coefficients $\lambda_\parallel$ and $\lambda_\perp$. The term $\lambda_\parallel$ represents the adiabatic component (along $\boldsymbol{M}$) of the spin polarization and $\lambda_\perp$ represents the anomalous Hall effect for the vorticity.

B. Miscroscopic calculation

Here we calculate the spin density induced by the electric field based on the model of spin-orbit interaction due to heavy impurities of Sec. III B. The spin density polarized along direction α induced by the electric field along the k direction is written as $s^\alpha = s^\alpha_k E_k$, where s^α_k is the linear response coefficient. The dominant contribution arises from the same diagram as in Fig. 4(a) with the left vertex replaced by a Pauli matrix, which reads

$$s^\alpha_k(\boldsymbol{q}) = \frac{e}{V^3}\frac{i}{\pi}\frac{\lambda n_{\rm i} v_{\rm i}{}^3}{m}\mathrm{Re}\sum_{\boldsymbol{k}\boldsymbol{k}'} k'_k\left[\left(\boldsymbol{k}'+\frac{\boldsymbol{q}}{2}\right)\times\left(\boldsymbol{k}+\frac{\boldsymbol{q}}{2}\right)\right]_\beta \mathrm{tr}\left[\sigma_\alpha g^{\rm r}_{\boldsymbol{k}+\frac{\boldsymbol{q}}{2}}\sigma_\beta g^{\rm r}_{\boldsymbol{k}'+\frac{\boldsymbol{q}}{2}} g^{\rm a}_{\boldsymbol{k}'-\frac{\boldsymbol{q}}{2}} g^{\rm a}_{\boldsymbol{k}''} g^{\rm a}_{\boldsymbol{k}-\frac{\boldsymbol{q}}{2}}\right]. \tag{59}$$

Using Eq. (34), we obtain

$$\begin{aligned}
s^\alpha_k(\boldsymbol{q}) &= s^{{\rm sh},\alpha}_k(\boldsymbol{q}) + \delta_{\alpha,z}s^\parallel_k(\boldsymbol{q}) + \epsilon_{\alpha\beta z}s^\perp_k(\boldsymbol{q}),\\
s^{{\rm sh},\alpha}_k(\boldsymbol{q}) &= \frac{e}{V^3}\frac{i}{\pi}\frac{\lambda n_{\rm i} v_{\rm i}{}^3}{m}\mathrm{Re}\sum_{\boldsymbol{k}\boldsymbol{k}'\boldsymbol{k}''} k'_k[\boldsymbol{k}'\times\boldsymbol{k}]_\alpha \sum_{\sigma=\pm} g^{\rm r}_{\boldsymbol{k}+\frac{\boldsymbol{q}}{2},\sigma} g^{\rm r}_{\boldsymbol{k}'+\frac{\boldsymbol{q}}{2},-\sigma} g^{\rm a}_{\boldsymbol{k}'-\frac{\boldsymbol{q}}{2},-\sigma} g^{\rm a}_{\boldsymbol{k}'',-\sigma} g^{\rm a}_{\boldsymbol{k}-\frac{\boldsymbol{q}}{2},-\sigma},\\
s^\parallel_k(\boldsymbol{q}) &= \frac{e}{V^3}\frac{i}{\pi}\frac{\lambda n_{\rm i} v_{\rm i}{}^3}{m}\mathrm{Re}\sum_{\boldsymbol{k}\boldsymbol{k}'\boldsymbol{k}''} k'_k[\boldsymbol{k}'\times\boldsymbol{k}]_z \sum_{\sigma=\pm} \left(g^{\rm r}_{\boldsymbol{k}+\frac{\boldsymbol{q}}{2},\sigma} - g^{\rm r}_{\boldsymbol{k}+\frac{\boldsymbol{q}}{2},-\sigma}\right) g^{\rm r}_{\boldsymbol{k}'+\frac{\boldsymbol{q}}{2},\sigma} g^{\rm a}_{\boldsymbol{k}'-\frac{\boldsymbol{q}}{2},\sigma} g^{\rm a}_{\boldsymbol{k}'',\sigma} g^{\rm a}_{\boldsymbol{k}-\frac{\boldsymbol{q}}{2},\sigma},\\
s^\perp_k(\boldsymbol{q}) &= \frac{e}{V^3}\frac{i}{\pi}\frac{\lambda n_{\rm i} v_{\rm i}{}^3}{m}\mathrm{Re}(-i)\sum_{\boldsymbol{k}\boldsymbol{k}'\boldsymbol{k}''} k'_k[\boldsymbol{k}'\times\boldsymbol{k}]_\beta \sum_{\sigma=\pm} \sigma g^{\rm r}_{\boldsymbol{k}+\frac{\boldsymbol{q}}{2},\sigma} g^{\rm r}_{\boldsymbol{k}'+\frac{\boldsymbol{q}}{2},-\sigma} g^{\rm a}_{\boldsymbol{k}'-\frac{\boldsymbol{q}}{2},-\sigma} g^{\rm a}_{\boldsymbol{k}'',-\sigma} g^{\rm a}_{\boldsymbol{k}-\frac{\boldsymbol{q}}{2},-\sigma}.
\end{aligned} \tag{60}$$

After summation over the wave vectors, the coefficients in Eq. (58) are obtained as

$$\begin{aligned}
\lambda_{\rm sh} &= e\frac{\pi^2}{3}\frac{\lambda n_{\rm i} v_{\rm i}{}^3}{m^2}\tau\frac{4M^2-\frac{1}{\tau^2}}{\left(4M^2+\frac{1}{\tau^2}\right)^2}\sum_{\sigma\sigma'}\nu_\sigma k_{F\sigma}^2\nu_{\sigma'}^2 k_{F\sigma'}^2,\\
\lambda_\parallel &= e\frac{\pi^2}{3}\frac{\lambda n_{\rm i} v_{\rm i}{}^3}{m^2}(-2\tau)\sum_\sigma\left[\nu_\sigma^3 k_{F\sigma}^4\tau^2 + \nu_\sigma^2 k_{F\sigma}^2\sum_{\sigma'}\nu_{\sigma'}k_{F\sigma'}^2\frac{\left(4M^2-\frac{1}{\tau^2}\right)}{\left(4M^2+\frac{1}{\tau^2}\right)^2}\right],\\
\lambda_\perp &= e\frac{\pi^2}{3}\frac{\lambda n_{\rm i} v_{\rm i}{}^3}{m^2}\frac{-4M}{\left(4M^2+\frac{1}{\tau^2}\right)^2}\sum_{\sigma\sigma'}\nu_\sigma k_{F\sigma}^2\nu_{\sigma'}^2 k_{F\sigma'}^2\sigma'.
\end{aligned} \tag{61}$$

In the disordered case with $M\tau \gg 1$, the order of magnitude of each term is

$$\lambda_{\rm sh} \sim \frac{\epsilon_{\rm so}}{k_F{}^2}\frac{1}{M^2},\quad \lambda_\parallel \sim \frac{\epsilon_{\rm so}}{k_F{}^2}\tau^2,\quad \lambda_\perp \sim \frac{\epsilon_{\rm so}}{k_F{}^2}\frac{1}{M^3\tau}, \tag{62}$$

meaning that the adiabatic spin polarization is dominant, while the spin Hall effect dominates the perpendicular component. In the limit of $M=0$, $\lambda_{\rm sh}$ representing the spin-vorticity coupling and spin Hall effect remains finite, while $\lambda_\parallel$ and $\lambda_\perp$ vanish.

C. Vorticity-induced torque

In ferromagnets, the vorticity-induced spin, Eq. (58), generates a current-induced torque near surfaces given by

$$\begin{aligned}
\boldsymbol{T}_\omega &= \lambda_{\rm sh}M\gamma[\hat{\boldsymbol{M}}\times(\nabla\times\boldsymbol{E})]\\
&\quad + \lambda_\perp M\gamma[\hat{\boldsymbol{M}}\times[\hat{\boldsymbol{M}}\times(\nabla\times\boldsymbol{E})]],
\end{aligned} \tag{63}$$

where $\gamma \equiv \frac{e}{m}$ is the electron gyromagnetoratio. This is a kind of so-called spin-orbit torque [29] arising from inhomogenuity of current. In ferromagnets with $M\tau \gg 1$ and $M/\epsilon_F = O(1)$, the first term dominates, as seen from Eqs. (62). Interestingly, the coefficient $\lambda_{\rm sh}$ does not depend on τ in this regime, resulting in a universal torque when written in terms of the applied field $\boldsymbol{E}$. Although current-induced torques on magnetic textures have been discussed intensively [29], the effect of vorticity and inhomogeneous current density has not been focused on. It is of interest to confirm experimentally the correlation between the vorticity-induced torque and the spin Hall effect, both determined by the coefficient $\lambda_{\rm sh}$.

Let us compare the vorticity-induced torque to the so-called β-torque [39,40] induced by spin relaxation and magnetization structure,

$$\boldsymbol{T}_\beta = \beta a^3[\hat{\boldsymbol{M}}\times(\boldsymbol{j}\cdot\nabla)\hat{\boldsymbol{M}}], \tag{64}$$

where β is a small constant representing the rate of spin relaxation and a is the lattice constant. Its magnitude in common ferromagnets is typically of the order of $\beta \sim (M\tau_{\rm sf})^{-1}$, where $\tau_{\rm sf}^{-1} \sim \epsilon_{\rm so}^2/\epsilon_F$ in the case of spin-orbit interaction [30,41]. In terms of the field E, $\boldsymbol{T}_\beta = \frac{e}{k_F{}^2}\tilde{\beta}[\hat{\boldsymbol{M}}\times(\boldsymbol{E}\cdot\nabla)\hat{\boldsymbol{M}}]$, where $\tilde{\beta} \equiv \frac{k_F{}^2}{e}\beta a^3\sigma_{\rm e} \sim \widetilde{\epsilon_{\rm so}}^2\epsilon_F\tau$, with $\widetilde{\epsilon_{\rm so}} \equiv \epsilon_{\rm so}/\epsilon_F$. Thus the ratio of the torque and the field is $\boldsymbol{T}_\beta/E \sim \frac{e}{k_F{}^2\ell_M}\widetilde{\epsilon_{\rm so}}^2\epsilon_F\tau$, while for the vorticity-induced torque it is $\boldsymbol{T}_\omega/E \sim \frac{e}{k_F{}^2\ell_\omega}\widetilde{\epsilon_{\rm so}}$, where ℓ_M is the length scale of the magnetization structure and ℓ_ω is the length scale of surface vorticity in the case of ohmic fluid. Considering the fact that the β torque is second order in the spin-orbit interaction [30], while the vorticity torque

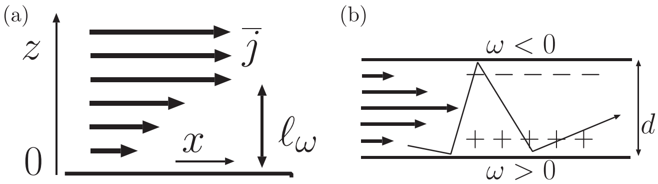

FIG. 5. (a) Schematic figure showing the current profile near the boundary (chosen as $z = 0$). Vorticity is finite in the length scale of ℓ_ω, where the current density changes. (b) Schematic figure showing vorticity-induced spin relaxation mechanism due to electron diffusion. The sign denotes the direction of vorticity $\boldsymbol{\omega}$. Electron diffusion is represented by a zigzag line.

is linear, surface vorticity may have a crucial role in current-induced torques. An even stronger effect is expected when surface roughness is considered, as roughness would enhance generation of vorticity. Nucleation of magnetic domain wall and skyrmion by artificial notches [42] would be carried out by the vorticity-induced torque as argued in Ref. [12]. Taking account of diffusion of electron, the spin density of Eq. (58) is modified to be long-ranged as [18]

$$\boldsymbol{s}(\boldsymbol{r}) = \int d^3r' D_s(\boldsymbol{r}-\boldsymbol{r}')[\lambda_{\rm sh}\boldsymbol{\omega}(\boldsymbol{r}') + \lambda_\parallel \hat{\boldsymbol{M}}(\hat{\boldsymbol{M}}\cdot\boldsymbol{\omega}(\boldsymbol{r}')) + \lambda_\perp(\hat{\boldsymbol{M}}\times\boldsymbol{\omega}(\boldsymbol{r}'))], \tag{65}$$

where $D_s(\boldsymbol{r}) \equiv \frac{1}{\tau}\sum_{\boldsymbol{q}} \frac{e^{i\boldsymbol{q}\cdot\boldsymbol{r}}}{Dq^2+\frac{1}{\tau_s}}$ is a diffusion propagator of electron spin, D and τ_s are the diffusion constant and spin relaxation time of electron, respectively. The electron spin diffusion length is $\ell_s \equiv \sqrt{D\tau_s}$. In the disordered case, therefore, the vorticity-induced torque is determined by the vorticity average over the spin diffusion length, $\overline{\boldsymbol{\omega}}$. Let us consider the case where ℓ_s is larger than the surface depth where the vorticity is finite, ℓ_ω. Choosing the axis as in Fig. 5(a), local vorticity of current density $\boldsymbol{j}$ is $\omega_y^{(j)} = \partial_z j_x$ and its average is

$$\overline{\omega}_y^{(j)} = \frac{1}{\ell_\omega}\int_0^{\ell_\omega} dz\partial_z j_x = \frac{\overline{j}_x}{\ell_\omega}, \tag{66}$$

where $\overline{j}_x$ is the current far from the surface and j_x at the surface ($z = 0$) is assumed to vanish. The averaged torque near the surface,

$$\overline{\boldsymbol{T}}_\omega = \lambda_{\rm sh} M\gamma(\hat{\boldsymbol{M}}\times\overline{\boldsymbol{\omega}}) + \lambda_\perp M\gamma[\hat{\boldsymbol{M}}\times(\hat{\boldsymbol{M}}\times\overline{\boldsymbol{\omega}})], \tag{67}$$

is therefore

$$\overline{\boldsymbol{T}}_\omega = \frac{M\gamma}{\sigma_{\rm e}}\left[\frac{\lambda_{\rm sh}}{\ell_\omega}[\hat{\boldsymbol{M}}\times(\hat{z}\times\overline{\boldsymbol{j}})] + \lambda_\perp[\hat{\boldsymbol{M}}\times[\hat{\boldsymbol{M}}\times(\hat{z}\times\overline{\boldsymbol{j}})]]\right], \tag{68}$$

where $\hat{z}$ denotes the direction normal to the surface. The torque represented by $\lambda_{\rm sh}$ has the same form as the one due to the surface Rashba-Edelstein effect, which induces spin polarization proportional to $\hat{z}\times\boldsymbol{j}$ [43].

For thin films as in Fig. 3, the vorticity-induced torque points opposite on the upper and lower plane and has no bulk effects.

D. Vorticity-induced spin relaxation

The vorticity-induced torque is naturally inhomogeneous, and would lead to spin relaxation effects. Let us consider a thin film [Figs. 3 and 5(b)] of thickness d with electric field parallel to the magnetization. The vorticity is then perpendicular to $\boldsymbol{M}$. The vorticity-induced torque drives the electron spin as

$$\dot{\boldsymbol{s}} = \gamma[\lambda_{\rm sh}(\boldsymbol{s}\times\boldsymbol{\omega}) + \lambda_\perp(\boldsymbol{s}\times\hat{\boldsymbol{M}})(\hat{\boldsymbol{M}}\cdot\boldsymbol{\omega}) + \lambda_\perp[\boldsymbol{s}\times(\hat{\boldsymbol{M}}\times\boldsymbol{\omega})]], \tag{69}$$

and thus the electron spin polarized along $\boldsymbol{M}$ gets flipped in a timescale of $(\lambda_{\rm sh}\omega)^{-1}$ [neglecting $\lambda_\perp(\ll\lambda_{\rm sh})$]. In a thin film, vorticity $\boldsymbol{\omega}$ arising from inhomogeneous flow points opposite on the upper and lower surfaces [Fig. 5(b)]. If calling the length scale where vorticity is finite measured from the surface as ℓ_ω [in the ohmnic fluid, $\ell_\omega \simeq \ell$ (mean-free path)], $2\ell_\omega/d$ of the total electron spins are disturbed by the vorticity-induced torque. The vorticity-induced spin relaxation time is therefore estimated as

$${\tau_\omega}^{-1} = \frac{\ell_\omega}{d}\lambda_{\rm sh}\omega, \tag{70}$$

assuming that the spin diffusion length is longer than d. Its magnitude is ${\tau_\omega}^{-1} \sim \widetilde{\epsilon_{\rm so}}\frac{eE}{k_F}\frac{1}{k_F d}$, assuming $\omega \sim E/\ell_\omega$. For $E = 10^{-2}$ V/μm and ${k_F}^{-1} \sim a = 10^{-10}$m, $\frac{eE}{k_F} = 10^{-6}$ eV $= 2\times 10^8$ Hz. Let us define a damping constant as $\alpha_\omega \equiv {\tau_\omega}^{-1}t_M$, where t_M is the timescale of magnetization dynamics. For ${t_M}^{-1} \sim 1$ GHz, the above estimate leads to $\alpha_\omega \sim 0.2\times\frac{\widetilde{\epsilon_{\rm so}}}{k_F d}$. For a large spin-orbit metal of a thin film, in particular, with surface roughness, the vorticity-induced relaxation may dominate over the intrinsic Gilbert damping. Experimentally, vorticity-induced damping would be separable from other isotropic intrinsic origins by using the anisotropic nature, i.e., vorticity-induced damping is suppressed if $\boldsymbol{E}\perp\boldsymbol{M}$.

V. VORTICITY-INDUCED INVERSE SPIN HALL EFFECT

Spin-current generation by fluid vorticity in a pipe was discussed in Ref. [10], and the inverse spin Hall voltage due to the spin current and measured on heavy metal leads was argued. In the case of the Hagen-Poiseuille flow considered there, the generated spin current is in the radial direction with spin polarization perpendicular to both radian and pipe directions and the inverse spin Hall voltage is along the flow.

The vorticity-induced inverse spin Hall effect is studied in the present context by calculating the spin-neutral force density (motive force for electric charge), taking account of the spin-orbit interaction to second order in the absence of M. The inverse spin Hall voltage here is an intrinsic one without leads of heavy metals, and would not apply to experimental situations with heavy metal leads.

The spin Hall coefficient $\lambda_{\rm sh}$ is a coefficient of the correlation function of spin and charge current density linear in the external wave vector [18]. The inverse spin Hall effect is represented as

$$\boldsymbol{j} = \lambda_{\rm ish}(\nabla\times\boldsymbol{B}_\omega), \tag{71}$$

where $\lambda_{\rm ish}$ is a coefficient proportional to $\lambda_{\rm sh}$ and $\boldsymbol{B}_\omega$ is an effective magnetic field that drives spin density [18]. In the

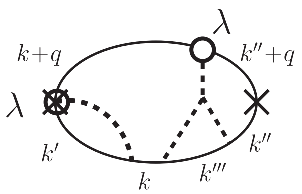

FIG. 6. Feynman diagram representing the vorticity-induced inverse spin Hall effect at the second order of the spin-orbit interaction (λ). The anomalous velocity vertex gives rise to an antisymmetric component of the momentum flux density that describes inverse spin Hall current, Eq. (71).

vorticity-driven case, the effective field is induced by the vorticity as

$$\boldsymbol{B}_\omega = \frac{\lambda_{\rm sh}}{\chi}\boldsymbol{\omega}, \tag{72}$$

where χ is spin susceptibility. In the ohmic regime, the relation Eq. (71) indicates that there is a motive force $\boldsymbol{f}^{\rm a}$ acting on electron charge that is proportional to the rotation of vorticity, $\nabla\times\boldsymbol{\omega}$. The inverse spin Hall motive force is therefore represented by an antisymmetric component of the momentum flux density for charge (spin neutral), $\pi^{\rm a}_{ij} = \xi^{\rm a}\epsilon_{ijk}a_k$, with a constant $\xi^{\rm a}$ and a vector $\boldsymbol{a}$, as $\boldsymbol{f}^{\rm a} = -\xi^{\rm a}(\nabla\times\boldsymbol{a})$, resulting in an inverse spin Hall current $\boldsymbol{j}\propto(\nabla\times\boldsymbol{a})$. As has been argued [34] [see also Eq. (3)], an antisymmetric component arises from vorticity, $\boldsymbol{a}\propto\boldsymbol{\omega}$. We thus obtain the inverse spin Hall current $\boldsymbol{j}\propto\nabla\times\boldsymbol{\omega}$, consistent with Eqs. (71) and (72). Let us confirm this fact by a microscopic calculation of spin-neutral momentum flux density $\pi_{ij}\equiv\langle\hat{p}_i\hat{v}_j\rangle\equiv\pi_{ijk}E_k$ in the case of $M=0$, including the spin-orbit interaction to second order. Obviously, the skew-scattering contribution is symmetric with respect to i and j [27] and the antisymmetic contribution arises from the side-jump contribution, whose dominant contribution is (shown in Fig. 6) [$^{\rm (sj)(2)}$ denotes the side-jump process at the second order of the spin-orbit interaction]

$$\begin{aligned}\pi^{\rm (sj)(2)}_{ijk}(\boldsymbol{q}) &= \frac{1}{4\pi V^4}\frac{\lambda^2 v_{\rm i}^5 n_{\rm i}^2}{2m} i\epsilon_{\alpha jl}\epsilon_{mn\beta}\\ &\quad\times\sum_{\boldsymbol{k}\boldsymbol{k}'\boldsymbol{k}''\boldsymbol{k}'''}(k'+k+q)_i\left(k''+\frac{q}{2}\right)_k(k'-k)_l k_n k''_m i\\ &\quad\times {\rm Imtr}\big[g^{\rm r}_{\boldsymbol{k}'}\sigma_\alpha g^{\rm a}_{\boldsymbol{k}+\boldsymbol{q}}\sigma_\beta g^{\rm a}_{\boldsymbol{k}''+\boldsymbol{q}} g^{\rm r}_{\boldsymbol{k}''} g^{\rm r}_{\boldsymbol{k}'''} g^{\rm r}_{\boldsymbol{k}}\big].\end{aligned} \tag{73}$$

The antisymmetric component of $\pi^{(2)}_{ij}$ is written in terms of a vector $\boldsymbol{a}_\omega$ as $\pi^{(2){\rm a}}_{ij} = \epsilon_{ijk}a_{\omega,k}$, where

$$\begin{aligned}\boldsymbol{a}_\omega &= \xi^{(2)}_\omega\boldsymbol{\omega},\\ \xi^{(2)}_\omega &= \frac{\pi}{12}\left(\frac{\epsilon_{\rm so}}{\epsilon_F}\right)^2 D\tau^2 v_{\rm i} = \lambda_{\rm sh}\left(\frac{\epsilon_{\rm so}}{\epsilon_F}\right)(v_{\rm i}\tau)\epsilon_F.\end{aligned} \tag{74}$$

The inverse spin Hall field induced by vorticity is therefore

$$\boldsymbol{E}_\omega = -\nabla\times\boldsymbol{a}_\omega = -\xi^{(2)}_\omega\nabla\times\boldsymbol{\omega}. \tag{75}$$

The inverse spin Hall voltage due to the vorticity-induced spin current in the present situation is therefore along the applied field $\boldsymbol{E}$, like the case with leads [16]. We note that the inverse spin Hall voltage in reality would be mixed with contributions from the symmetric components of the momentum flux density (see argument in Sec. II).

VI. SUMMARY AND DISCUSSION

We have explored the effects of vorticity of electron flow in ferromagnetic metals on the spin transport based on a hydrodynamic viewpoint. The spin-resolved momentum flux density was discussed, extending the results for anomalous Hall fluid studied previously in Ref. [27]. We have argued that the anomalous Hall contributions to the momentum flux density are written in terms of a troidal moment, $\boldsymbol{T}_{\boldsymbol{M}} = \boldsymbol{M}\times\boldsymbol{E}$, which acts as an effective driving field. When electron spin is taken into account, the spin-resolved momentum flux density π^α_{ij} (i and j represent the spatial direction and α denotes spin direction) are characterized by the three contributions, namely, the adiabatic contribution where spin $\boldsymbol{s}$ is parallel to $\boldsymbol{M}$, the nonadiabatic contribution written by $\boldsymbol{s}_\perp\equiv\boldsymbol{s}-\hat{\boldsymbol{M}}(\hat{\boldsymbol{M}}\cdot\boldsymbol{s})$ and a contribution written by $\tilde{\boldsymbol{s}}\equiv\boldsymbol{s}\times\boldsymbol{M}$. The troidal moment $\boldsymbol{T}_{\boldsymbol{M}}$ is therefore extended to include two nonadiabatic contributions, $\boldsymbol{T}_{\boldsymbol{s}_\perp}\equiv\boldsymbol{s}_\perp\times\boldsymbol{E}$ and $\boldsymbol{T}_{\tilde{\boldsymbol{s}}}\equiv\tilde{\boldsymbol{s}}\times\boldsymbol{E}$. Those results were confirmed by linear response calculations in a model with the impurity-induced spin-orbit interaction.

The spin-resolved force density $-\nabla_j\pi^\alpha_{ij}$, or spin motive force, was argued and roles of electron vorticity on the motive force were discussed. Besides the conventional conservative force due to spin-vorticity coupling, proportional to $\nabla(\boldsymbol{s}\cdot\boldsymbol{\omega})$ ($\boldsymbol{\omega}$ is the vorticity), there is a nonconservative force, proportional to $\nabla\times(\boldsymbol{\omega}\times\boldsymbol{s}) = (\boldsymbol{s}\cdot\nabla)\boldsymbol{\omega}$. Like spin current, the spin-resolved momentum flux density and force density are physical conserved currents and their definitions are not unique.

Spin density induced by vorticity was calculated and direct and inverse spin Hall effects were argued in the context of the spin-vorticity coupling. The vorticity-induced damping near the surface and interface was discussed. The torque arises from the homogeneity of the current (or total field), in contrast to conventional current-induced relaxation torques such as β torque arising from inhomogeneous magnetization. The vorticity-induced torque is a linear effect of spin-orbit interaction, while the conventional relaxation torque is second order, meaning that vorticity effects may dominate in thin films. The effect leads to torque and relaxation localized near surfaces and interfaces. Spin Hall-induced spin-orbit torque was explained in terms of the spin-vorticity coupling. The inverse spin Hall effect due to the vorticity-induced spin current was shown to be described by the antisymmetric part of the momentum flux density evaluated at the second order of the spin-orbit interaction.

We considered the case of uniform magnetization with inhomogenuity of the applied electric field. For a complete discussion of the troidal moment, inhomogeneous magnetization needs to be taken into account. For this future work, an effective gauge field approach [38] is expected to be useful.

ACKNOWLEDGMENT

The author thanks H. Funaki and R. Toshio for valuable discussions. This paper was supported by a Grant-in-Aid for

Scientific Research (B) (No. 21H01034) from the Japan Society for the Promotion of Science.

APPENDIX A: DERIVATION OF MOMENTUM FLUX DENSITY OF EQS. (29) and (30)

Here we derive the expression for the spin-resolved momentum flux density by evaluating the time derivative of the spin-resolved momentum. (See Ref. [27] for a simpler spinless case.) The Heisenberg equation for field representation of spin-resolved momentum $\dot{p}_i^\alpha$ (i and α are the directions of momentum and spin, respectively) reads $\dot{p}_i^\alpha = i\langle [H, c^\dagger \hat{p}_i \sigma_\alpha c]\rangle$, where $[A, B] \equiv AB - BA$ is a commutator. The contribution from the spin-orbit coupling is focused. The commutator is calculated using $\nabla_i^r \delta(\boldsymbol{r}-\boldsymbol{r}') = -\nabla_i^{r'} \delta(\boldsymbol{r}-\boldsymbol{r}')$ and integral by parts as

$$
\begin{aligned}
i[H_{\rm so}, (c^\dagger \hat{p}_i \sigma_\alpha c)_{\boldsymbol{r}}] &= -\frac{i}{4}\lambda \int d\boldsymbol{r}' \epsilon_{jkl} \big(\nabla_j^{r'} V(\boldsymbol{r}')\big)\big[c^\dagger(\boldsymbol{r}')\sigma_l(\nabla_k c(\boldsymbol{r}')) - (\nabla_k c^\dagger(\boldsymbol{r}'))\sigma_l c(\boldsymbol{r}'), c^\dagger(\boldsymbol{r})\sigma_\alpha(\nabla_i c(\boldsymbol{r})) - (\nabla_i c^\dagger(\boldsymbol{r}))\sigma_\alpha c(\boldsymbol{r})\big] \\
&= -\frac{i}{2}\lambda\big[(\nabla_j V)[-\epsilon_{jk\alpha}\nabla_k[c^\dagger \overleftrightarrow{\nabla}_i c] + i\epsilon_{jkl}\epsilon_{l\alpha\beta}[c^\dagger\sigma_\beta \overleftrightarrow{\nabla}_i (\nabla_k c) - (\nabla_k c^\dagger)\sigma_\beta \overleftrightarrow{\nabla}_i c]] \\
&\quad + (\nabla_i\nabla_j V)[-\epsilon_{jk\alpha}(c^\dagger \overleftrightarrow{\nabla}_k c) + i\epsilon_{jkl}\epsilon_{l\alpha\beta}\nabla_k[c^\dagger\sigma_\beta c]]\big] \\
&= -\nabla_j \hat{\pi}_{ij}^{\mathrm{so},\alpha} + \hat{f}_{s,i}^\alpha,
\end{aligned} \tag{A1}
$$

where

$$
\hat{\pi}_{ij}^{\mathrm{so},\alpha} = \frac{i}{2}\lambda\big[(\nabla_k V)\epsilon_{jk\alpha}[c^\dagger \overleftrightarrow{\nabla}_i c] - i(\nabla_i\nabla_k V)\epsilon_{jkl}\epsilon_{l\alpha\beta}(c^\dagger\sigma_\beta c)\big], \tag{A2}
$$

$$
\hat{f}_{s,i}^\alpha = \frac{i}{2}\lambda\big[(\nabla_i\nabla_j V)\epsilon_{jk\alpha}(c^\dagger \overleftrightarrow{\nabla}_k c) - i(\nabla_j V)\epsilon_{jkl}\epsilon_{l\alpha\beta}[c^\dagger\sigma_\beta \overleftrightarrow{\nabla}_i (\nabla_k c) - (\nabla_k c^\dagger)\sigma_\beta \overleftrightarrow{\nabla}_i c]\big] \tag{A3}
$$

are the spin-orbit contributions to the momentum flux density and force density, respectively.

The contribution of the kinetic term, $\hat{\pi}_{ij}^{K,\alpha}$, is similarly calculated, and the total momentum flux density operator is

$$
\begin{aligned}
\hat{\pi}_{ij}^{K,\alpha} + \hat{\pi}_{ij}^{\mathrm{so},\alpha}(\boldsymbol{r},t) &= c^\dagger\left[\frac{1}{m}\hat{p}_i\hat{p}_j\sigma_\alpha - \lambda(\nabla_k V)\epsilon_{jk\alpha}\hat{p}_i + \frac{1}{2}\lambda(\nabla_i\nabla_k V)(\delta_{j\alpha}\delta_{k\beta} - \delta_{j\beta}\delta_{k\alpha})\sigma_\beta\right]c \\
&\equiv \hat{\pi}_{ij}^{s,\alpha}
\end{aligned} \tag{A4}
$$

whose expectation value is Eqs. (29) and (30). The hydrodynamic equation for spin transport is therefore Eq. (28).

The fact that the time derivative of the spin-resolved momentum density is not written in terms of conserved current in the presence of spin relaxation, in the same way as the case of spin current. This means that the momentum flux density cannot be defined uniquely. In other words, spin-resolved momentum density is not physical observable. In this paper, we use the form of Eq. (A2). Different definitions result in different values of viscosity constants. We note, however, that physical quantities like spin density are uniquely defined as in the spin current case [18].

[1] M. N. Baibich, J. M. Broto, A. Fert, F. Nguyen Van Dau, F. Petroff, P. Etienne, G. Creuzet, A. Friederich, and J. Chazelas, Giant Magnetoresistance of (001)Fe/(001)Cr Magnetic Superlattices, Phys. Rev. Lett. **61**, 2472 (1988).

[2] T. Valet and A. Fert, Theory of the perpendicular magnetoresistance in magnetic multilayers, Phys. Rev. B **48**, 7099 (1993).

[3] L. Berger, Low-field magnetoresistance and domain drag in ferromagnets, J. Appl. Phys. **49**, 2156 (1978).

[4] L. Berger, Possible existence of a Josephson effect in ferromagnets, Phys. Rev. B **33**, 1572 (1986).

[5] L. Berger, Emission of spin waves by a magnetic multilayer traversed by a current, Phys. Rev. B **54**, 9353 (1996).

[6] J. C. Slonczewski, Current-driven excitation of magnetic multilayers, J. Magn. Magn. Mater. **159**, L1 (1996).

[7] G. Tatara, H. Kohno, and J. Shibata, Microscopic approach to current-driven domain wall dynamics, Phys. Rep. **468**, 213 (2008).

[8] M. Matsuo, J. Ieda, E. Saitoh, and S. Maekawa, Effects of Mechanical Rotation on Spin Currents, Phys. Rev. Lett. **106**, 076601 (2011).

[9] M. Matsuo, Y. Ohnuma, and S. Maekawa, Theory of spin hydrodynamic generation, Phys. Rev. B **96**, 020401(R) (2017).

[10] M. Matsuo, E. Saitoh, and S. Maekawa, Spin-mechatronics, J. Phys. Soc. Jpn. **86**, 011011 (2017).

[11] R. J. Doornenbal, M. Polini, and R. A. Duine, Spin–vorticity coupling in viscous electron fluids, J. Phys.: Mater. **2**, 015006 (2019).

[12] J. Fujimoto, W. Koshibae, M. Matsuo, and S. Maekawa, Zeeman coupling and Dzyaloshinskii-Moriya interaction driven by electric current vorticity, Phys. Rev. B **103**, L220402 (2021).

[13] S. J. Barnett, Magnetization by rotation, Phys. Rev. **6**, 239 (1915).

[14] A. Einstein and W. J. de Haas, Experimenteller Nachweis der Ampereschen Molekularströme, Verh. Dtsch. Phys. Ges. **17**, 152 (1915).

[15] R. F. Snider and K. S. Lewchuk, Irreversible thermodynamics of a fluid system with spin, J. Chem. Phys. **46**, 3163 (1967).
[16] M. Matsuo, J. Ieda, E. Saitoh, and S. Maekawa, Spin-dependent inertial force and spin current in accelerating systems, Phys. Rev. B **84**, 104410 (2011).
[17] R. Takahashi, M. Matsuo, M. Ono, K. Harii, H. Chudo, S. Okayasu, J. Ieda, S. Takahashi, S. Maekawa, and E. Saitoh, Spin hydrodynamic generation, Nat. Phys. **12**, 52 (2016).
[18] G. Tatara, Spin correlation function theory of spin-charge conversion effects, Phys. Rev. B **98**, 174422 (2018).
[19] M. Dyakonov and V. I. Perel, Possibility of orienting electron spins with current, Sov. Phys. JETP Lett. **13**, 467 (1971).
[20] J. E. Hirsch, Spin Hall Effect, Phys. Rev. Lett. **83**, 1834 (1999).
[21] T. Scaffidi, N. Nandi, B. Schmidt, A. P. Mackenzie, and J. E. Moore, Hydrodynamic Electron Flow and Hall Viscosity, Phys. Rev. Lett. **118**, 226601 (2017).
[22] G. M. Gusev, A. D. Levin, E. V. Levinson, and A. K. Bakarov, Viscous transport and Hall viscosity in a two-dimensional electron system, Phys. Rev. B **98**, 161303(R) (2018).
[23] R. Gurzhi, Minimum of resistance in impurity-free conductors, Zh. Eksp. Teor. Fiz. **44**, 771 (1963) [JETP **17**, 521 (1963)].
[24] A. C. Keser, D. Q. Wang, O. Klochan, D. Y. H. Ho, O. A. Tkachenko, V. A. Tkachenko, D. Culcer, S. Adam, I. Farrer, D. A. Ritchie, O. P. Sushkov, and A. R. Hamilton, Geometric Control of Universal Hydrodynamic Flow in a Two-Dimensional Electron Fluid, Phys. Rev. X **11**, 031030 (2021).
[25] R. Toshio, K. Takasan, and N. Kawakami, Anomalous hydrodynamic transport in interacting noncentrosymmetric metals, Phys. Rev. Research **2**, 032021(R) (2020).
[26] H. Funaki and G. Tatara, Hydrodynamic theory of chiral angular momentum generation in metals, Phys. Rev. Research **3**, 023160 (2021).
[27] H. Funaki, R. Toshio, and G. Tatara, Vorticity-induced anomalous Hall effect in an electron fluid, Phys. Rev. Research **3**, 033075 (2021).
[28] S. Conti and G. Vignale, Elasticity of an electron liquid, Phys. Rev. B **60**, 7966 (1999).
[29] A. Manchon, J. Železný, I. M. Miron, T. Jungwirth, J. Sinova, A. Thiaville, K. Garello, and P. Gambardella, Current-induced spin-orbit torques in ferromagnetic and antiferromagnetic systems, Rev. Mod. Phys. **91**, 035004 (2019).
[30] H. Kohno, G. Tatara, and J. Shibata, Microscopic calculation of spin torques in disordered ferromagnets, J. Phys. Soc. Jpn. **75**, 113706 (2006).
[31] K. M. D. Hals and A. Brataas, Phenomenology of current-induced spin-orbit torques, Phys. Rev. B **88**, 085423 (2013).
[32] F. Freimuth, S. Blügel, and Y. Mokrousov, Berry phase theory of Dzyaloshinskii-Moriya interaction and spin-orbit torques, J. Phys.: Condens. Matter **26**, 104202 (2014).
[33] L. D. Landau and E. M. Lifshitz, *Fluid Mechanics*, 2nd ed. (Butterworth-Heinemann, Oxford, 1987).
[34] S. R. D. Groot and P. Mazur, *Non-Equilibrium Thermodynamics* (Dover Books on Physics, New York, 2011).
[35] A. Stern, Berry's Phase, Motive Forces, and Mesoscopic Conductivity, Phys. Rev. Lett. **68**, 1022 (1992).
[36] J. Shi, P. Zhang, D. Xiao, and Q. Niu, Proper Definition of Spin Current in Spin-Orbit Coupled Systems, Phys. Rev. Lett. **96**, 076604 (2006).
[37] P. Coleman, *Introduction to Many-Body Physics* (Cambridge University Press, Cambridge, 2015).
[38] G. Tatara, Effective gauge field theory of spintronics, Physica E **106**, 208 (2019).
[39] S. Zhang and Z. Li, Roles of Nonequilibrium Conduction Electrons on the Magnetization Dynamics of Ferromagnets, Phys. Rev. Lett. **93**, 127204 (2004).
[40] A. Thiaville, Y. Nakatani, J. Miltat, and Y. Suzuki, Micromagnetic understanding of current-driven domain wall motion in patterned nanowires, Europhys. Lett. **69**, 990 (2005).
[41] G. Tatara and P. Entel, Calculation of current-induced torque from spin continuity equation, Phys. Rev. B **78**, 064429 (2008).
[42] X. Z. Yu, D. Morikawa, K. Nakajima, K. Shibata, N. Kanazawa, T. Arima, N. Nagaosa, and Y. Tokura, Motion tracking of 80-nm-size skyrmions upon directional current injections, Sci. Adv. **6**, eaaz9744 (2020).
[43] V. Edelstein, Spin polarization of conduction electrons induced by electric current in two-dimensional asymmetric electron systems, Solid State Commun. **73**, 233 (1990).